ACTIVE GALACTIC NUCLEI ACTIVITIES AND FLOW OF RELATIVISTIC JETS

By

Abdissa Tassama

Supervisor: Tolu Biressa (Ph.D Fellow)

THESIS SUBMITTED IN PARTIAL FULFILLMENT OF THE
REQUIREMENTS FOR THE DEGREE OF
MASTER OF SCIENCE IN PHYSICS
(ASTROPHYSICS)
AT
JIMMA UNIVERSITY
COLLEGE OF NATURAL SCIENCES
JIMMA,ETHIOPIA
JUNE 2019

JIMMA UNIVERSITY

PHYSICS

The undersigned hereby certify that they have read and recommend to the College of Natural Sciences for acceptance a thesis entitled "**ACTIVE GALACTIC NUCLEI ACTIVITIES AND FLOW OF RELATIVISTIC JETS**" by **Abdissa Tassama** in partial fulfillment of the requirements for the degree of **Master of Science in Physics(Astrophysics)**.

Dated: June 2019

Supervisor:
_____
Tolu Biressa (Ph.D Fellow)

External Examiner:
_____
Dr. Solomon Belay

Internal Examiner:
_____
Dr. Tamirat Ababe

Chairperson:
_____

JIMMA UNIVERSITY

Date: **June 2019**

Author: **Abdissa Tassama**

Title: **ACTIVE GALACTIC NUCLEI ACTIVITIES AND FLOW OF RELATIVISTIC JETS**

Department: **Physics**

Degree: **MSc.**
Convocation: **June**
Year: **2019**

_____
Signature of Author

To My Family

Table of Contents

List of Tables

List of Figures

_____

Abstract

The astrophysics of Active Galactic Nuclei (AGN) is one of the long outstanding issues in searches among the scientific communities raised with diverse perspectives like nebula, quasars, etc some decades ago. Currently, this exotic system is at least understood as the center of an active galaxy. Thus, the consensus of this recent theory has opened up a number of research issues for the progress of astrophysical science including how the hosting galaxy evolves with the AGN, how matter and energy flow towards and outwards, etc. Moreover, most of the AGNs possess Supermassive Black Holes (SMBHs) and accrete matter at a very high rate as current observations report. Consequently, both observations of Electromagnetic (EM) spectrums and Gravity Waves (GWs) will be considered to provide complementary information about the AGNs and the roles in their environments including black holes in their centers, outflow and inflow of matter-energy. Interested with this background rationale, we study the mechanisms of AGN interaction with its environment and flow of relativistic jets where General Relativistic (GR) Magneto-hydrodynamic (MHD) equations and kerr metric are being considered. The solutions of the field equations are treated with a metric that involves charged systems for the possible relativistic jets including accretions. Then, numerical data is being generated using the latest version Mathematic software. Finally, the theoretical data is being compared with that of observation for validation of the model. Where flat disk accretion model is considered. Due to rotation and atmosphere of the AGN a pressure supported tori and radiation transfer is exploited.

Key words: Accretion, AGN, GR, MHD, Metric, SMBH, EMW, GWs, matter-energy-flow, relativistic-jets.

_____

Acknowledgement

First and foremost I would like to thank the only Omnipotent God, who help me starting from my mother womb to still. I would like to express my dearest gratitude to my supervisor Tolu Biressa (Ph.D fellow) for all his encouragement, support, and helpful suggestions. His generosity, kindness and encouragement have kept me going through the most difficult of times. In fact, I always felt lucky having him as a supervisor. It was always a pleasure to talk to him discussing scientific questions. He taught me style of physics. I am also grateful to co-supervisor Mr.Milkessa G.(M.Sc)for all his constructive comments. I have had the fortune of having many an excellent discussions during various collaborations with him. My sincere thanks to Dinka T. and Lachisa A. from the beginning for their encouragement and contribution for this success.

_____

Chapter 1

Introduction

1.1 Scheme of the thesis

In this introductory chapter we provide the detail background of the work including literature reviews/issues thereof, objectives and methods. In chapter 2 the background physics, General Relativity theory (GR) is previewed. In chapter 3 overview of AGN, such as basic concept and definitions, highlights of existing models, AGN activity and its environment. In chapter 4 we develop boundary conditions and then derive dynamical equations that are used to describe the system. This chapter is intended to enrich the method and model going to be implemented. In chapter 5 we provide discuss and results of the work. In the final chapter, chapter 6 summary and conclusions be given.

1.2 Background and literature review

Active galactic nuclei (AGNs) are the luminous objects in the universe. Their source of luminosity is central region of a galaxy, and the most probable engine of the activity is the supermassive black hole in the center of the host galaxy. The observed AGNs can be divided into several classes: quasars, Seyfert galaxies, radio galaxies, and BL Lacertae objects. On a more general level, AGNs can be classified as radio-loud and radio-quiet AGNs.

Observationally, the discovery of Active Galactic Nuclei (AGN) goes back to more than a century ago where the first spectroscopic detection of emission lines from the nuclei of NGC 1068 and

Messier 81 was reported by Fath (1909) and the discovery of the jet in Messier 87 by Curtis (1918). Then, a number of further spectroscopic studies were carried out by astronomers in the presence of unusual emission lines in some galaxy nuclei with less understanding. However, the systematic study of galaxies with nuclear emission lines began with the work of Seyfert (1943). Carl Seyfert (1943) studied the spectra of spiral nebulae in detail and found that a fraction of them have bright nuclei and emission lines. Based on the observed properties, Seyfert 1 and Seyfert 2 galaxies are today used as an AGN classification due to optical spectra Carl seyfert selected group of galaxies on basis of high central surface brightness (i.e stellar appearing cores). Seyfert obtained spectra of these galaxies and found that the optical spectra of several of these galaxies (NGC 1068, NGC 1275, NGC 3516, NGC 4151 and NGC 7469) are dominated by high excitation nuclear emission lines. Seyfert galaxies received no further attention until 1955, when NGC 1068 and NGC 1275 were detected as radio sources.

Some year later, radio astronomer discovered a class of extremely bright radio sources that appeared to be associated with optical point sources Matthews and Sandage (1963). The development of radio astronomy during 1950s was one of the key initiatives in understanding AGN including the detected active elliptical radio source galaxies such as Messier 87 and Centaurus Bolton Minkowski and Baade. Consequently, further progress in radio survey led to the discovery of new radio sources as well as identifying the visible-light sources associated with the radio emission Zwicky (1967). In photographic images, some of these objects were nearly point-like or quasi-stellar objects (QSOs) in appearance, and were classified as quasi-stellar radio sources (later abbreviated as quasars,).

Also, further advances in the discovery of AGNs were stepped up in optically strong ultraviolet continuum through and later in infrared and X-ray surveys during the 1960s Markarian (1967), Weedman (1973). In fact this period was a breakthrough in the spectrum analysis where an accurate position of certain quasars like 3C 273 were obtained observationally. Remarkably, during 1970s both ground-based and sky-based observational techniques were developed to analyse wide range of the QSOs spectral distribution that covers almost all spectrum of the electromagnetic radiation.

Conclusions were drawn that the spectrum of QSOs is just identical to that of the nuclei of the Seyferts. Later studies vastly have shown that both objects are recognized as the nuclei of hosting galaxies, the AGN. Moreover, all massive galaxies are likely to have hosted AGN activity during their lifetimes. As of the current understanding AGNs are among the most powerful energy sources in the Universe with extreme luminosity over the whole electromagnetic spectrum.

After widespread studies of active galactic centers,researchers of the field come to a common consensus that the plausible reason for the extreme luminosity in some galactic centers is the presence of compact object (like black hole) in galactic center which accretes materials close to it. Accreting materials (collection of; stars, dusts and gases), release tremendous amount of gravitational potential energy in the form of radiation. This existing supermassive blackhole in center of AGN is the present standard theories. The appealing AGNs with Super-Massive Black Holes at their centers powered with accretion Caputi (2014a). However the central gravitating black hole can be either rotating or non-rotating by itself. Accretion onto non-rotating black hole is omni-directional, while accretion onto rotating black is confined to equatorial plane perpendicular to the black hole's rotation axis. however in evidences almost all black holes are rotating so that we have accreting materials confined in equatorial plane and form disk-like structure called accretion disk. Accordingly, there is a plethora of research going on modeling of these exotic systems with various approaches and perspectives. In fact, there are encouraging developments where some of the models are successful within their limits. The present computing standard theories are appealing AGNs with Super-Massive Black Holes at their centers powered with accretion, see Caputi (2014b) and the references therein. However, there are unsettled debates on the mechanisms how these central engines affect the dynamistic of systems in their environments, for example see Best and Heckman (2012), Gaspari (2015), Nixon et al. (2012).

So motivated by this scientific rationale we are interested to study the role of AGN activity in generation and collimation of the outflow and flow of relativistic jets.

1.3   Statement of the problem

The astrophysics of AGN is one of the long standing issues that was in frequent searches among the scientific communities raised with diverse perspectives like nebula, quasars , etc some decades ago. Currently, this exotic system is at least understood as the center of an active galaxy. Since, the consensus of this recent theory a lot of issues are currently open to research for the progress of the astrophysical science that include how the hosting galaxy evolves with respect it, how do matter and energy flow towards and outwards, testing the effect of gravity, etc.

Research questions

- In what way does the AGN affect systems around its environment?

- What is the geometry of interaction system of the AGN with its environment?

- In what way does the AGN intake and eject relativistic jets and radiate?

1.4   Objectives

1.4.1   General objective

To study active galactic nuclei activities and flow of relativistic jets.

1.4.2   Specific objectives

- To explain the way that AGN affects systems around its environment.

- To describe the geometry of interaction system of the AGN with its environment.

- To study the way AGN intake system from its environment and release relativistic jets and radiation.

1.5   Methodology

General relativistic field equation is being used to derive the relevant dynamical equations with simplifying boundary conditions. The central engine of the AGN is considered with SMBH. It is hoped to work for both in the presence or absence of such real object, where in the later case a pseudo SMBH is assumed. The rational behind is that, the AGN is presumably sufficiently massive whether it is cored with such objects or not to appeal for strong gravity around its environment. On top of this the general consensus that the AGNs cores are being rotating is presumed, so that the space time around the AGNs is Kerr geometry. Due to more mass inflow, a fat disk accretion model is considered. Moreover, due to rotation and atmosphere of the AGN a pressure supported tori and radiation transfer is exploited. The derived equations are expected to correlate the process occurred at emission to that of observation point far away from the AGN by the general covariant transformation.

Chapter 2

Introduction to General theory of relativity and Einstein Field Equations in Kerr spacetime

General Relativity is the geometrical theory of gravitation, work of Albert EinsteinEinstein (1915). It unifies Special Relativity and Sir Isaac Newton's law of universal gravitation with the insight that gravitation is not due to a force but rather a manifestation of curved space and time, with the curvature being produced by the mass-energy and momentum content of the space-time. General Relativity is the most widely accepted theory of gravitation and has important astrophysical implications. The fields such as detection of light rays in the gravitational field of massive stars, the gravitational red-shift, gravitational time delay and others were most successfully explained by General Theory of relativityTewari (1988). Under the normal conditions the general relativistic effects are very small and extremely difficult to detect.

The philosophy of General Relativity (GR) states, the effect of gravitation is contained in the metric tensor field $g_{\mu\nu}$. Thus, in Einstein's theory of gravity, the gravitational field is promoted to a space-time metric $g_{\mu\nu}$. In 1916 Schwarzschild constructed the first exact solution of Einstein's gravitational field equationsSchwarzschild (1916). His solution was one of the physically interpretable solutions of Einstein's field equations. Schwarzschild metric tensor field is that due to a static spherically symmetric body situated in empty space such as the Sun or a star. Schwarzschild

metric has been the basis of theoretical investigations of gravitational phenomena in Einstein's theory of gravitation. This is in spite of the fact that the Sun and most planetary bodies in the Solar System are not perfectly spherical but oblate spheroidal in shape.

2.1 Einstein Field Equation (EFE)

The Einstein field equation is;

$$R_{\mu\nu} - \frac{1}{2}g_{\mu\nu}R + g_{\mu\nu}\lambda = -kT_{\mu\nu} \tag{2.1.1}$$

where $R_{\mu\nu}$ and R are Ricci-tensor and scalar curvature respectively constructed from an invariant 4-rank Riemann curvature tensor which is given as;

$$R^\lambda_{\mu\lambda\nu} = \Gamma^\lambda_{\mu\lambda}, \nu - \Gamma^\lambda_{\mu\nu}, \lambda + \Gamma^\eta_{\mu\lambda}\Gamma^\lambda_{\eta\nu} - \Gamma^\eta_{\mu\nu}\Gamma^\lambda_{\eta\lambda} \tag{2.1.2}$$

and also $T_{\mu\nu}$ is the stress-Energy tensor, $g_{\mu\nu}$ is metric and λ is cosmological constant and $k = \frac{8\pi G}{c^4}$. The christoffelsymbol is given as;

$$\Gamma^\mu_{\lambda\nu} = g^{\rho\mu}(g_{\rho\mu,\nu} + g_{\rho\nu,\mu} - g_{\mu\nu,\rho}) \tag{2.1.3}$$

In our case the cosmological constant neglected. so the EFE equation rewrite as;

$$R_{\mu\nu} - \frac{1}{2}g_{\mu\nu}R = -kT_{\mu\nu} \tag{2.1.4}$$

By contracting the indices of equation (2.1.4) we will get the following which is called curvature scalar

$$R_{\mu\nu} - \frac{1}{2}g_{\mu\nu}R = -kT_{\mu\nu} \tag{2.1.5}$$

$$R - 2R+ = -kT \tag{2.1.6}$$

$$R = kT \tag{2.1.7}$$

By substituting R in equation (2.1.4)

$$R_{\mu\nu} = -k(T_{\mu\nu} - \tfrac{1}{2}g_{\mu\nu}T) \tag{2.1.8}$$

2.2 Spherically symmetric solutions of EFEs

Karl Schwarzschild was investigate the exact solution of Einstein's field equations was found in 1916. This solution describes the geometry of space-time outside a spherically symmetric matter distribution. Schwarzschild obtained the solution for static and spherically symmetric gravitational field produced by non-rotating neutral black hole. The existence of the solution have play a great role in astrophysical situations such as involving spherical accretion , accretion disk structure around black hole and stars, their optical appearance etc. They have become an important part of the arsenal of astrophysicists. The most general spherically symmetric metric is

$$ds^2 = \alpha(r,t)dt^2 - \beta(r,t)dr^2 - \gamma(r,t)d\Omega^2 - \delta(r,t)dtdr \qquad (2.2.1)$$

where

$$d\Omega^2 = d\theta^2 + \sin^2\theta d\phi^2$$

2.3 Kerr metric

In order for a solution to be fit for the universe it is required that it must be asymptotically flat that is, the solution must tend to flat space metric at large distance. To describe a uniformly rotating bounded source, two or more variables must be used, and this complicates the process of finding an exact solution of EFE tremendously. Roy kerr discover such solution in 1963. This discovery is arguably one of an influential discoveries in second half of the 20th century as it has so impacts on different field of science such as physics, Astrophysics and astronomy. Roy Kerr obtained axially symmetric, stationary, but not static gravitational field produced by rotating neutral black hole. The Kerr metric, written in Boyer-Lindquist (BL) co-ordinates (oblate spheroidal co-ordinates), is given by

$$ds^2 = g_{tt}dt^2 + 2g_{t\phi}dtd\phi + g_{rr}dr^2 + g_{\theta\theta}d\theta^2 + g_{\phi\phi}d^2\phi \qquad (2.3.1)$$

where

$$g_{tt} = -(1 - \frac{2mr}{\rho^2})$$

$$g_{t\phi} = -\frac{2mar\sin^2\theta}{\rho^2}$$

$$g_{rr} = \frac{\rho^2}{\Delta}$$

$$g_{\theta\theta} = \rho^2$$

$$g_{\phi\phi} = \frac{\sin^2\theta}{\rho^2}[(r^2+a^2)^2 - \Delta a^2\sin^2\theta]$$

and

$$\rho^2 \equiv r^2 + a^2\cos^2\theta$$

$$\Delta^2 \equiv r^2 - 2Mr + a^2$$

Using equation (2.1.3), the non-zero christoffel components of kerr-metric are;

$$\Gamma^t_{tr} = \frac{M(r^2 + a^2)}{r^2 \Delta}$$

$$\Gamma^\phi_{tr} = \frac{Ma^2}{r^2 \Delta}$$

$$\Gamma^t_{t\theta} = -\frac{2Ma^2 \cos\theta}{r^3}$$

$$\Gamma^\phi_{t\theta} = -\frac{2Ma^2 \cos\theta}{r^3}$$

$$\Gamma^t_{r\phi} = -\frac{Ma(3r^2 + a^2)}{r^2 \Delta}$$

$$\Gamma^\phi_{r\phi} = \frac{r(\Delta - a^2 - ma^2)}{r^2 \Delta}$$

$$\Gamma^\phi_{\phi\theta} = (1 + \frac{2ma}{r^2}) \cos\theta$$

$$\Gamma^t_{\phi\theta} = \frac{2Ma^3 r \sin^3\theta \cos\theta}{\rho^4}$$

$$\Gamma^r_{tt} = \frac{\Delta M(2r^2 - \rho^2)}{\rho^4}$$

$$\Gamma^r_{t\phi} = -\frac{\Delta Ma(2r^2 - \rho^2) \sin^2\theta}{\rho^4}$$

$$\Gamma^r_{rr} = \frac{1 + \Delta/\rho^2)r - M}{\Delta}$$

$$\Gamma^r_{r\theta} = \Gamma^\theta_{\theta\theta} = \frac{\Gamma^\theta_{rr}}{\Delta} = -\frac{a^2 \sin 2\theta}{2\rho^2}$$

$$\Gamma^r_{\theta\theta} = \Delta\Gamma^\theta_{r\theta} = -\frac{r\Delta}{\rho^2}$$

$$\Gamma^r_{\phi\phi} = -\frac{\Delta(r\rho^4 - a^2 M(2r^2 - \rho^2)) \sin^2\theta}{\rho^6}$$

$$\Gamma^\theta_{tt} = -\frac{a^2 Mr \sin 2\theta}{\rho^6}$$

$$\Gamma^\theta_{t\phi} = \frac{aMr \sin 2\theta(r^2 + a^2)}{\rho^6}$$

$$\Gamma^\theta_{\phi\phi} = -\frac{\sin 2\theta[(r^2 + a^2)\rho^4 + 2Ma^2 r(\rho^2 + (r^2 + a^2)) \sin^2\theta]}{2\rho^6}$$

10

Chapter 3

Introduction to Active galactic nuclei (AGN)

Since 1940 a newly developing science in astrophysics and still mystery is AGN and its system. An AGN is a compact region at the center of a galaxy, characterized by exceptionally bright observed luminosities across the entire electromagnetic spectrum far in excess of what can produced by the host galaxy's stars alone. Many different classes of AGN are present with having different observational properties. The demonstration of these classes are different ratios of radio, optical/UV and X-ray flux, dissimilar amounts of variability and the presence or absence of broad and narrow emission lines in their optical spectra. The study of multi-wavelength of AGN and their corresponding yields unification model of AGN.

3.1   Structure and unification model of AGN

Even if diverse types of AGN are observed with different properties, it is generally believed that their fueling mechanisms are essentially similar. The current AGN model unification scheme between this different types of AGN were developed by Antonucci (1993) and Urry and Padovani (1995). Antonucci (1993) defined a preliminary simple model of two basic types of AGN: radio quiet and radio loud. Seyfert galaxies and radio-quiet quasars belong to the radio-quiet group, while radio galaxies, radio-loud quasars, and BL Lac objects make the radio-loud group. Urry and Padovani
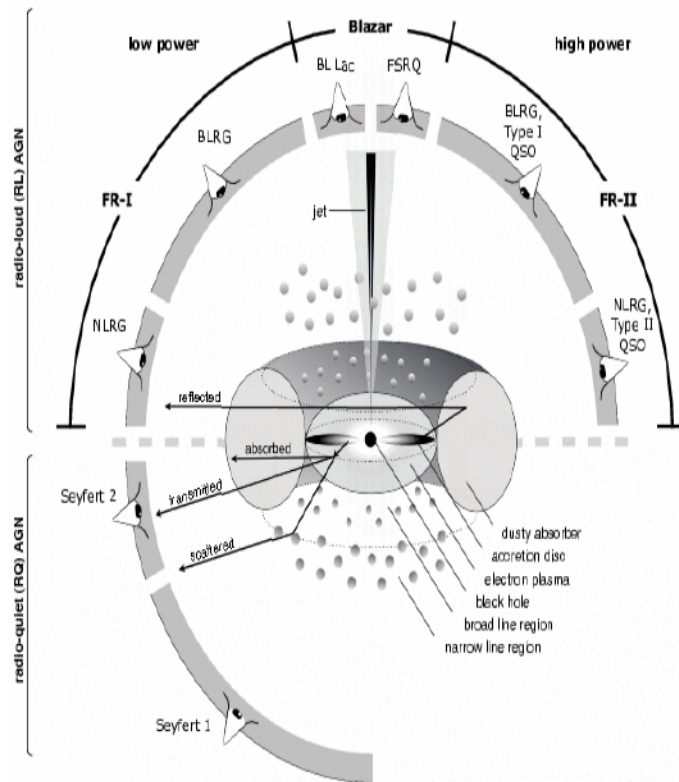
Figure 3.1: Beckmann and Shrader (2012);graphic by Marie-Luise Menzel

(1995) further divided the radio-loud subclass into two intrinsically different types based on their radio luminosity: the high-luminosity sources, such as radio-loud quasars and FR II radio galaxies, and the low-luminosity sources, such as BL Lac objects and FR I radio galaxies. With this division, all AGNs belong in one of three physically different types. Differences between AGN in each of these types are caused by different viewing angles from which we observe them. Depending orientation of the dusty torus to the observers line of sight, Type 1 AGN are usually observed face-on through a cavity in the torus and are typically bright in the X-ray, UV, and optical spectrum; Type 2 AGN may be intrinsically less luminous or are observed at an angle through the torus, and are thereby obscured by high column densities of dust and gas from the observers line of sight, enough so that most or all of the X-ray emission is absorbed and undetected Aird et al. (2012), Lanzuisi et al. (2014).

AGN model manifest the central engine is a super-massive black hole, surrounded by an accretion disk. Above the accretion disk there are broad emission line gas clouds, at a few fractions of a parsec (pc) from the central black hole, which are heated by radiation from the disk, giving rise to broad optical/UV emission lines. Close to the disk plane is the molecular/dust torus at around. There are also the narrow emission line clouds. This model contains the essence of the components, yet their linear dimension and the distance to the central black hole are approximate, depending greatly on the AGN's luminosity Krolik (1999). Actually the mass accretion rate determine the strength of radiation pressure force. Hence, at very high mass accretion rates the radiation pressure force becomes so great that the inner disk expands vertically and can no longer be treated as geometrically thin. In accretion onto the black hole there are also collimated out flows in the form of a pair of large scale relativistic jets which are directed along the spin axis of the accretion disk.

The observed widths of spectral lines in various wavebands are the estimator of the distances to the structures of AGN. As accretion disk widen to molecular torus, the material outside the equatorial plane cannot be in orbit as within half an orbital period it would intersect the disk. The conjecture is that it must be within some form of outflowing wind, which has speed of order of the escape velocity. However, even if the outflowing material is not in the form of a wind, the difference between the escape velocity and the velocity due to Keplerian motion is logarithmically small compared to the uncertainties for the use of the escape velocity and the ionisation parameter to constrain the location of structure in AGN Blustin et al. (2005). These crude distance estimators are enough to determine that the broad line region may be due to material evaporating off the accretion disk or molecular torus, and that the narrow line region is much further out.

At inclinations further away from the jet axis, or where there is no jet from the central engine, observers will be able to observe emission from the accretion disk. In many systems, the emission manifests as a big blue bump in the optical/UV part of the spectrum. The emission lines from the broad and narrow line regions are also seen in the optical spectrum. Objects with this viewing geometry are known as Seyfert I and steep-spectrum radio quasars (SSRQs) are normally radio

lobe-dominated radio quasars. Their lobe emission dominates their core emission, since beaming effects are less severe as their relativistic jets are viewed at larger inclination angles.

At even higher inclinations the molecular torus blocks the line of sight to the accretion disk. The only observable is scattered light from the central engine. The scattered light is polarised. At these inclinations even the broad line emission region may be obscured, but the narrow emission line region remains unobscured. If the narrow line region is visible, but the broad line region is not, then the objects are classed as Seyfert 2s and are predominantly radio-quiet.

It is believed that atleast 10% of AGN the accelerating region produce collimated jets of material that extend for distance of kiloparsecs. This large scale jets appear to be typically associated with giant elliptical galaxies and denoted radio loud galaxies. Radio loud AGN are further subdivided into quasars which has high luminosity and Blazars with BL Lac type objects are therefore classed as Faranoff-Riley (FR-I)sources which have extended jets but a brighter central source. Quasars may have a brighter radio lobes extend to kiloparsec. Because the lobes are brighter at radio frequency than the central sources this objects fall into the FR-II source classification Fanaroff and Riley (1974). FR-I radio lobes are edge-dim and centrally bright, with a relativistic jet which gradually widens into the lobe. FR-II radio lobes are edge-bright and centrally dimmer, with a relativistic jet which maintains its narrow cross-section until the lobe. FR-II radio jets also tend to have a hot spot on the side furthest from the galaxy. This hot-spot is the strong shock where the relativistic jet terminates, colliding with a wall of ambient thermal gas.

3.2 AGN activity and its environment

AGN produce an enormous amount of energy that is injected into their surrounding environment through ionizing radiation and relativistic jets. Also the comoving density evolution of AGN is remarkably similar to the evolution of the total star formation rate density and to the evolution of the space density of starbursting galaxies. One of the key roles in the framework of galaxy formation is the AGN activity.

In essence, all nearby galaxies possess a super-massive black hole at their center, and that the black hole mass is correlated with the bulge mass and velocity dispersion also suggest a strong link between galaxy formation and black hole growth (ie AGN activity). This imply that the black hole and the bulge grow together until the AGN is luminous enough so that the radiative pressure drives winds that expel the cold gas in the intergalactic medium thereby stopping the star formation **?**. This is AGN feedback, in the form of radiative pressure. This self-regulating process which links the energy released by the AGN to the surrounding gaseous medium and in this way, impacting on the evolution of the host galaxy.

The AGN activity (SMBH growth)and galaxy growth are co-evolutionary processes. These processes may regulate each other over time to produce the galaxy and SMBH sizes we observe today. It is believed that AGN activity and star formation are interconnect. Both central black hole growth and star formation rely on the abundance of cold molecular gas, while cold dust and gas collapse to trigger star formation, the SMBH at the galaxy core gravitationally attracts cold gas and dust into a clumpy obscuring reservoir a few parsecs out from the SMBH, which fuels a thin, hot SMBH accretion disk with a radius typically ≤ 1 pc. Since AGN activity also produces X-rays, the expectation is that AGN should track strong dust emission and that X-ray and infrared emission should be correlated.

Fundamentally, the rates of star formation and BH growth in galaxies will be down to the balance between feeding (a supply of cold gas) and feedback (the prevention of the cold gas supply). A simple explanation for the co-evolution of star formation and BH growth and the observed relationships between galaxies and BHs, is that they grow from a common fuel supply. Both star formation and AGN activity are known to be a source of energy and momentum (due to radiation pressure and the expulsion of material through winds or jets). If these winds, jets or radiation pressure are able of significantly suppress the supply of cold gas they will be the cause of negative feedback. If either one of these processes injects energy or momentum into their surroundings (i.e., provides the source of heating or outfows) future AGN activity and star formation could be enhanced or suppressed (i.e.,

the impact). The overall results of these processes could affect the observed properties of galaxies, BHs and the gas in the larger scale environment. The AGN activity can directly impact upon the evolution of their host galaxies. The potential impact of AGN activity can be simply assessed by considering the amount of energy it takes to build a massive black hole:

$$E_{BH} \quad = \quad \eta M_{BH} c^2 \tag{3.2.1}$$

Where η is the mass-to-energy efficiency conversion, M_{BH} is mass of Black hole and C is speed of light.

Several studies have been taken on the nearby environments of different types of AGN have been made using the spatial galaxy-galaxy cross-correlation amplitude B_{gg}Bahcall and Spitzer Jr (1969). Different researchers are differentiating the AGN environment using this the spatial galaxy-galaxy cross-correlation amplitude (B_{gg}). For example the study result of **?** implies that, for Seyfert 2 galaxies are close to their control sample of nonactive galaxies, while Seyfert 1 galaxies were less clustered. The other parameters that determine the difference in environment of seyfert 1 and 2 is their interaction with the neighboring galaxies which could drive more molecular gas toward the center of the galaxy, and thus increasing obscuration Dultzin-Hacyan et al. (1999).

As different showed usual environment for quasars is a small group of galaxies, although some of them may also be found in richer clusters. Radio-loud quasars tend to have higher clustering in their environment than the radio quiet quasars Ellingson et al. (1991), Fisher et al. (1996), Yee and Green (1984). They suggest that this difference may be due to more efficient fueling for quasars in rich environments, causing triggering of radio-loud quasars only in rich environments. Radio galaxies are found in high-density environments. The environment of radio galaxies depend on their radio power and redshift Hill and Lilly (1991). Some consensus imply that the redshift dependency is stronger for FR II type galaxies than for those with FR I type morphology. At redshift $z \sim 0$, FR I radio galaxies are found in slightly richer environments than the FR II. Because sources with higher power can be detected from a larger distance, the differences caused by redshift cannot be

separated from differences caused by power.

On the other hand large-scale environments of AGNs provide for a test of the unification model. The orientation of the nucleus does not depend on the group of galaxies, or even large-scale environment in which its host galaxy resides. The environmental studies have provided evidence against the unification model. BL Lac objects have local environments more typical to FR II type radio galaxies and radio-loud quasars than to FR I radio galaxies. This suggests that FR I galaxies may not be the parent population of BL Lac objects as the unified scheme predicts and also detected characteristics more typical to FR II radio galaxies in the radio emission of some BL Lac objects Kharb et al. (2010). These findings included extended luminosities and hot spots that are often found in radio-loud quasars. Based on these findings, it is possible that BL Lac objects may not constitute a homogeneous population that fits in the simple unified scheme. Instead, BL Lac objects may have both, FR I and FR II galaxies as their parent population.

In general, the differences between the environments of different types of AGN are moderately connected to the types of AGN host galaxies. The hosts of radio galaxies are red elliptical galaxies in dense environments,and for Seyfert galaxies, are spiral galaxies in lower densities. According to Hickox presented, radio and X-ray selected AGNs are clustered similarly to their host galaxy populations, but infrared-selected AGNs are weakly clustered relative to a matched galaxy sample Hickox et al. (2009). These findings suggest that different types of AGN are likely to be triggered in different environments. Based on the luminosity-density field we found that a typical environment for Seyfert galaxies and quasars is a void or a low-density filament. Radio galaxies are more likely to be in superclusters. BL Lac objects are also often in high-density environments, but their fraction in void environments is higher than that of radio galaxies.

AGN feedback is the (self-regulating) process which links the energy released by the AGN to the surrounding gaseous medium and in this way, impacting on the evolution of the host galaxy. The energy injected by the AGN can provide the mechanism, either by preventing the cooling of gas or by expelling gas from the galaxy, to quench star formation (thus limiting the number of

17

massive galaxies) and to limit the growth of the SMBH. Thus, it helps explaining key observations in these areas obtained in the recent years Mizuta et al. (2004). In addition, the energy dumped in the environment of the AGN affects the fuelling of the nuclear activity itself, thereby regulating its duty-cycle.

There are two modes in which AGN feedback can operate and they depend mostly on the type of nuclear activity. These are quasar mode and kinetic mode. The quasar (or radiative) mode is mostly associated with high luminosity AGN, i.e. those emitting close to the Eddington limit, where most of the energy is released by radiation (or a wind) from the accretion disk but where also radio jets can play a role. The release of energy drives gas outflows expelling gas from the galaxy. The jet (or kinetic) mode is, instead, considered to be dominant in low-power AGN where the radio plasma provids the main source of energy, preventing the gaseous atmosphere from cooling back into the galaxy. While in the most extreme cases high luminosity AGN and cool-core clusters the separation between the two modes can be clear-cut, in other more intermediate situations, and for the most common types of AGN, the separation may not be always so sharp. Multi-wavelengths observations are often needed to recognize and disentangle different modes of feedback. Furthermore, the luminosity (or radio power) of the AGN is not the only parameter defining the impact. The coupling between the energy released and the medium is important Blandford and Payne (1982) as well as the duty-cycle of the activity.

3.3   Rotating BH

The source of rotating black holes are thought to be the gravitational collapse of a massive rotating star or from the collapse of a collection of stars with an average non-zero angular momentum. This only exist if the radius of the collapsing body reaches the gravitational radius. Such collapses will be more general than a non-rotating collapse and would complete the case for all gravitational collapses. The asymmetry inherent in the collapsing body is suggested to be radiated gravitationally and the final outcome is assumed to be a stationary spherically symmetric rotating black hole.

All the features of rotating black holes can then be described by the charge,mass and the angular momentum of the black hole.

A complete mathematical description of space-time around a rotating black hole was provided by Roy Kerr in 1963. The Kerr metric used to describe a rotating black hole is studied using various coordinate systems out of which the Boyer Lindquist coordinates provide an extension to the Schwarzschild coordinates and are the most studied and exploited for the study of rotating space-time behavior. The angular velocity of the central black hole plays an important role in determining not only the space-time geometry exterior to it but also the dynamics of plasma fluid and the configuration of electromagnetic field. This motivates the theoretical astrophysicist to study rotating black holes which is mostly belongs to the Kerr-Newman family (i,e fully determined by mass, angular momentum and electric charge of the black hole). The source of this gravitational field is a charged mass current. For astrophysical black holes, the electric charge is supposed to be unimportant. The reason is that an electric charge would be compensated by electric currents i.e. plasma flows in the environment of the black hole. Hence, astrophysicists focus on rotating electrically neutral black holes. They are described by the Kerr solution.

The dynamics of a particle near a black hole is determined by the curvature of space- time around the black hole. Roy Kerr obtained axially symmetric, stationary, but not static gravitational field produced by rotating neutral black hole. Black holes' specific angular momentum $'a'$ of mass M and angular momentum J is given by; $a \equiv \frac{J}{M}$, where $G = c = 1$ and

$$a_* \equiv \frac{a}{M} = \frac{J}{M^2}$$

where a_* is the dimensionless parameter which is introduced to express the magnitude of the spin. Its' ranges is between -1 and 1. if $a_* = -1$ (maximally counter-rotating BH), through $a_* = 0$ (Schwarzschild BH), to $a_* = 1$ (maximally rotating BH). In his geometry of spacetime, adopted in Boyer-Lindquist coordinates the line element of an event has the form:

$$ds^2 = (\frac{4aM^2}{r}^2 \sin\theta - \rho^4 \Delta \Sigma^2 \rho^2) dt^2 + \frac{4Mr}{\rho^2 a \sin^2\theta} dt d\phi + \frac{\rho^2}{\Delta} dr^2 + \rho^2 d\theta^2 + \frac{\sum^2}{\rho^2 \sin^2\theta} d\phi^2 \ (3.3.1)$$

where

$$\rho^2 \equiv r^2 + a^2 \cos^2 \theta$$

$$\Sigma^2 \equiv (r^2 + a^2)^2 - a^2 \Delta \sin^2 \theta$$

$$\Delta^2 \equiv r^2 - 2Mr + a^2$$

and $'a'$ is the ratio of angular momentum(J) to unit mass of black hole(M). The units used in Kerr metric solution is geometrical units in which r, M and a have units of length. unlike schwarzschild, the mixed metric coefficients $g_{t\phi}, g_{\phi t}$ are non zero. Therefore, the metric is a non-diagonal metric irrespective of the choice of the coordinate system. The non vanishing non diagonal components of the Kerr metric introduces new concepts of space-time reversal and static limit which accounts for intriguing new physics in such spacetimes. The metric is stationarity and symmetricity is interconnect with respect to the polar axis of $\theta = 0$ and the equatorial plane $\theta = \frac{\pi}{2}$. The sign of the metric used here is (- + + +). let note that in studying about accretion disks it is convenient to write the Kerr metric in the approximate form valid close to the equatorial plane $\cos^2 \theta << 0$ and introduce the vertical cylindrical coordinate $z = r \cos \theta$. The determinant of the Kerr metric element given in above is;

$$-g = \rho^4 \sin^2 \theta \qquad (3.3.2)$$

$$\Rightarrow \sqrt{-g} = \rho^2 \sin \theta$$

In a general, Kerr solution is one possible realization for an axisymmetric and stationary spacetime. Each symmetry of a spacetime is associated with a Killing field. The higher the symmetry, the more Killing fields are available. Axisymmetry and stationarity lead to two Killing vectors: axisymmetry requires an asymptotically space like Killing field, $\partial \phi$, and stationarity requires an asymptotically timelike Killing field, ∂t. Both Killing fields can be extracted from the Killing equation for the spacetime. The advantage of this axial symmetry and stationarity of gravitational field of the central rotating black hole is greatly reduce the complexity of the governing equations. $\partial t g_{\mu\nu}$ = 0 and $\partial \phi g_{\mu\nu} = 0$ where stationarity and axial symmetricity respectively

20

The kerr black hole (rotating BH) has horizons and ergosphere. Event horizon is a surface that circumscribe the black hole, within which nothing can be seen and nothing can escape, because the necessary escape velocity would equal the speed of light. The event horizon acts like a kind of one-way membrane, means event horizon flags the point of no return for infalling matter, radiation and observers. The notion of an event horizon is justified because events or in relativistic language world points that are located beyond the horizon radius cannot be detected from outer observers. Like every horizon the black hole event horizon separates observable from unobservable objects.

Here, we focused on the outer event horizon neglecting inner horizon. The reason why the Cauchy horizon neglected is that it is of subordinate importance for astronomy because observational features stop naturally at the outer horizon. For vanishing spin parameter, $a = 0$, these two horizons degenerate to only one horizon, the Schwarzschild radius $R_s = 2M$. Generically, there is no dependence of any horizon radius on the poloidal angle θ. Hence, the horizons have in any cases spherical symmetry.

The other region around a Kerr black hole is where spacetime itself is dragged along in the direction of rotation at a speed greater than the local speed of light in relation to the rest of the universe. In this region, negative energy states are possible, which means that the rotational energy of the black hole can be tapped through various manifestations of the "Penrose process". Within this region the Killing vector field $k(\frac{\partial}{\partial t})$ becomes spacelike, which is a very different situation from the Schwarzschild case, where this only happens inside the event horizon. Of course this means another direction must have become timelike, and so as it turns out, inside the ergosphere any observer has to move with a certain minimum (nonzero) coordinate angular velocity.

The important point in defining the ergosphere is the region for which the Killing vector field k is spacelike. That is, if an observer inside the ergosphere would like to follow an orbit of k, it would have to move faster than light; an observer inside the ergosphere cannot remain stationary, eventhough the observer finds himself outside of the event horizon. The mathematical surface of ergosphere is defined by the vanishing component g_{tt} of the metric. Hence, the ergosphere depends
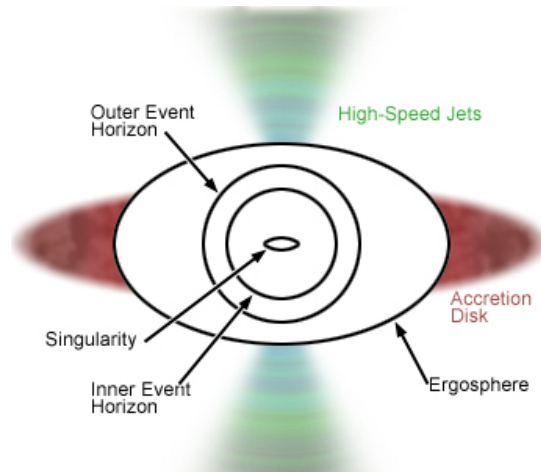
Figure 3.2: kerr black hole,2003 stuart J. Robbins

on the poloidal angle and has oblate morphology, comparable to the Earth. At the poles of the black hole, the ergosphere touches the outer event horizon. At the equator the ergosphere has a bulge(see figure3.2).

The key feature of the Kerr geometry is the rotation of space-time and here, the dynamics implies that reference frames are dragged. It is not possible to sustain static observers. Hence, the ergosphere is also called the static limit. There is no globally time-like non-rotating Killing field. Observers are also dragged by the rotating space-time. An observer with fixed (r, θ) with respect to the rotating frame of reference in the vicinity of the black hole will appear to be stationary in this frame of reference of the black hole however locally stationary observer will be rotating with respect to the asymptotic Lorentz frame.

3.4 Accretion disk

Accretion disks are the generic structures associated with compact objects powered by matter accretion onto them. Accretion may exist in different astrophysical objects such as AGN, newly formed

stars and proto-planets, binary star systems. Here, in this section we focus on the disks in AGNs. Their formation is a consequence of the fact that the specific angular momentum of the accreting matter at the outer boundary of the flow is larger than its Keplerian value on the accreting body vicinity. If the accreting matter conserves angular momentum but is free to radiate energy, it will lose energy until it is on a circular orbit of radius $R_c = J^2/(GM)$, where J is the specific angular momentum of the gas, and M is the mass of the accreting compact object. The role of the accretion disk is to rid this excess angular momentum of the disk plasma and allow it to accrete onto the gravitating compact object. This process is effected by viscous stresses which at the same time cause the heating of the accreting matter and emission of radiation with rather specific spectral characteristics. The geometry of accretion disk are; For non-rotating black hole the accretion of matters has spherical symmetry while accretion onto rotating black hole has axial symmetry (disk like structure perpendicular to the axis of rotating black hole). The geometry is determined moreover by the angular momentum.

The forces that acting on the accreting materials onto compact rotating objects are inward gravitational force, centrifugal force and outward radiative force (radiation from the innermost accreting matters). At certain region around gravitating object, the inward gravitational force is balanced by the two outward forces and hence the accreting matters orbit the central gravitating objects without falling in. This is known as stable orbit in which materials confined. However; it does not mean that this is the last fate of the accreting materials. The accreting materials at the innermost stable orbit have higher velocity compared to that of the outermost parts. This differential rotation leads to viscosity. Due to the action of viscosity, we expect energy and angular momentum to be transformed from the faster moving inner regions of the disk to the slower moving outer regions. As the materials in an inner layer loses angular momentum, it spirals inward and here viscosity determines the rate of radial inflow of matter and therefore the rate at which the gravitational potential energy is converted into other forms, like radiation. Materials had no viscosity implies that, there would be no release of gravitational energy after the formation of the disk. Mathematically the gravitational potential

energy released by the accreting materials around compact object is:$E_{accretion} = \frac{GMm}{r}$, where G, M, m, r represents gravitational constant, mass of central compact object, mass of accreting matter and radius of central compact object respectively.

3.4.1 Thin disk

There are two types of accretion of matter with high angular momentum on to a compact central object, central object with mass M_{BH}. when the rate of matter supplied from outside $\dot{M}_{out}$ is lower than critical one then, in most case a thin, disk like structure is formed and if the rate of matter supplied from outside is much faster than critical rate thick accretion disk is formed (accretion torus). where

$$\dot{M}_{crit} = L_{Edd} \frac{M_{BH}}{Eff(R_{in})c^2} = 3 \times 10^8 \frac{M_{BH}}{M_\odot} [\frac{M_{BH}}{M_\odot}]$$

where Under this subsection let we introduces thin accretion disk by considering the standard model accretion disk. The standard model of accretion disk was first formulated Shakura (1972)and then generalized to the Kerr- metric by Novikov and Thorne (1973). The central work of the α-model was to describe a geometrically thin non-self gravitating disk by hydrodynamical equations averaged over the disk thickness. Geometrically thin and non-self-gravitating disk means that the scale of height of the disk H (thickness) is much smaller than the radial distance r ($\frac{H}{r} << 1$) radial and vertical dependencies are separable. Working in cylindrical polar coordinates, the disk structure is most easily considered first in the z-direction. In addition, the disk is axisymmetric and stationary. The mass of the disk M_d is much smaller than the mass of the central object $M_c(M_d << M_c)$ so the gravitational influence of the disk is negligible. In this case the angular velocity will have the Keplerian form

$$\Omega(R) \quad = \quad \sqrt{\frac{GM}{R^3}} \tag{3.4.1}$$

where Ω is the angular velocity of the gas at radius R.

Most parameters can then be integrated vertically yielding surface densities which depend only
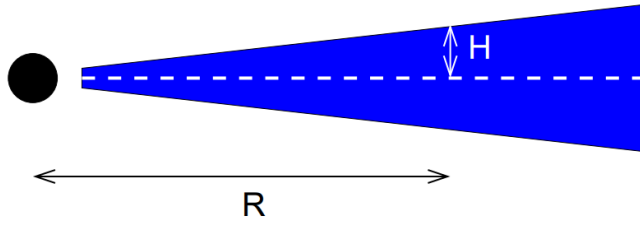
Figure 3.3: thin disk

on R and (α). For hydrostatic equilibrium in the vertical direction, the continuity equation gives

$$\frac{1}{\rho}\frac{\partial P}{\partial z} = \frac{\partial}{\partial z}\left[\frac{GM}{\sqrt{R^2+z^2}}\right] \tag{3.4.2}$$

where ρ is the density, P the pressure, and M is the mass of the central accreting object. R is the cylindrical radius, and z is the height out of the equatorial plane. For a thin disk $z << R$, it follows that

$$\frac{1}{\rho}\frac{\partial P}{\partial z} \simeq \frac{\partial}{\partial z}\left[\frac{GM}{R(1+\frac{1}{2}\frac{z^2}{R^2})}\right]$$

$$\simeq \frac{GMz}{R^3}$$

$$\frac{1}{\rho}\frac{\partial P}{\partial z} \simeq \frac{P}{H}$$

where H is a pressure scale-height, $z \sim H$, and

$$P = \rho c_s^2$$

The disk scaleheight may be expressed as

$$\frac{H}{R} \simeq c_s\sqrt{\frac{R}{GM}} \tag{3.4.3}$$

In the condition $H << R$,

$$c_s \simeq \sqrt{\frac{R}{GM}} \tag{3.4.4}$$

25

Recalling the continuity equation the radial flow and angular momentum through the thin disk will be

$$\frac{\partial}{\partial r}(R\Sigma\nu_R) \quad = \quad 0 \tag{3.4.5}$$

where $\sum = \int \rho dz$ is the surface density of the disk and ν_R is the radial drift velocity. Note that $R\Sigma\nu_R$ is a conserved quantity in the mass conservation equation, representing the constant in flow of mass through each fluid element in the disk. The accretion rate that obtained after integrating this equation is

$$\dot{M} \quad = \quad -2\pi R\Sigma\nu_R \tag{3.4.6}$$

where - sign indicating that the total mass within the disk is decreasing. The total angular momentum lost when mass moves in unit time from $R + dR$ to R

$$\frac{dL}{dR} \quad = \quad \dot{M}\frac{d(R^2\Omega(R))}{dR} \tag{3.4.7}$$

Since L changes, accreting matter needs to lose angular momentum. which is performed by viscous forces exerting torques. The total torque is

$$G(R) \quad = \quad 2\pi\nu\Sigma R^3\frac{d\Omega}{dR} \tag{3.4.8}$$

The conservation of momentum (Balancing net torque and angular momentum loss) gives

$$\frac{\partial}{\partial R}(R^3\Omega\Sigma\nu_R) \quad = \quad \frac{\partial}{\partial R}(R^3\Sigma\nu\frac{\partial}{\partial R}\Omega) \tag{3.4.9}$$

Through integrating

$$\Omega\Sigma\nu_R \quad = \quad \Sigma\nu\frac{\partial}{\partial R}\Omega) \tag{3.4.10}$$

where this again yields a constant, $\frac{C}{2\pi}$ which is determined by the inner boundary condition of the disk. At some radius, say R_* the gas stops transporting angular momentum outwards and must

26

form a boundary layer with the central object, so $\frac{\partial \Omega}{\partial R} = 0$. The angular velocity at this radius is approximately Keplerian, thus

$$\Sigma \nu_R \sqrt{\frac{GM}{R_*^3}} \quad = \quad \frac{C}{2\pi R_*^3} \tag{3.4.11}$$

By rearranging and using value of $\dot{M}$, then the constant C is

$$C \quad = \quad -\dot{M}\sqrt{GMR_*} \tag{3.4.12}$$

After substitution

$$\nu\Sigma \quad = \quad \frac{\dot{M}}{3\pi}(1 - \sqrt{\frac{R_*}{R}}) \tag{3.4.13}$$

and

$$\nu_R \quad = \quad -\frac{3\nu}{2R}(1 - \sqrt{\frac{R_*}{R}})^{-1} \tag{3.4.14}$$

In the case of $R_* << R$, ν_R is proportional to $\frac{\nu}{R}$, which in the standard (α-disk)disk formulation is

$$\nu_R \sim \frac{\alpha c_s H}{R} << c_s \tag{3.4.15}$$

as $\alpha < 1$. The radial motion in the thin accretion disk model is therefore a slow inwards drift, much smaller than the supersonic Keplerian motion in the rotational direction. Rate of viscous dissipation are per unit area is

3.4.2   Geometrically thick accretion disk

During the radiation pressure balances the gravitational force the accretion rate, $\dot{M}$, becomes too large, so solution of of thin disk solution breaks down. Hence, large mass accretion rate results in high disk luminosity. Accretion tori rotating around black hole have super-Eddington luminosity.

$$L_E \quad = \quad \frac{4\pi GMm_pc}{\sigma_T} \tag{3.4.16}$$

This is the maximum luminosity that could be emitted by spherically accreting materials (plasma fluid)around non-rotating black hole. Defining the accretion rate that produces this luminosity as $\dot{M}_{crit}$, the equation for the disk scale height, H, becomes

$$\dot{M_{Edd}} = \frac{4\pi GMm_p}{c\eta\sigma_T} \approx 2.2(\frac{0.1}{\eta})(\frac{M}{10^8 M_{\odot}}) \tag{3.4.17}$$

where $'\eta'$ is the ratio of the gravitational energy released to the rest energy. The ratio $'\eta'$ is 0.057 and 0.423 for Schwarzschild black hole and maximally rotating black holes respectively. Mass accretion rate and critical rate is a determinant luminosity of disk. These super-Eddington luminosities are observed in some active galactic centers that contains rotating black holes. Plasma fluid accretes spherically onto non-rotating black hole. The radiation released by in-falling plasma fluid is obscured by the spherically symmetric accretion. On the other hand, plasma fluid accreting onto rotating black hole is confined along the equatorial plane. That is, axial symmetry of the gravitational field confines the plasma fluid along equatorial plane. Then the radiation produced by the inflow of plasma fluid near the innermost stable orbit is not obscured or equatorially by the accreting plasma fluid. Thus the luminosity of the disk may exceeds Eddington luminosity. This reason may account for the observed super-Eddington luminosity in some active galaxies that dock rotating black holes in their centers.

Due to their specific shape (long, narrow funnels along the rotation axis) they are accelerate jets. So this is interesting in this thesis. Accretion tori differ from thin disks because all parameters need to be described in terms of both R and z. Vertically-integrated quantities are no longer physically meaningful. Furthermore, the α model of viscosity breaks down when $H \approx R$, causing the system of equations to be unclosed. Instead of viscosity we usually parametrise the angular velocity or angular momentum of the toroidal material. This is justified as the energy dissipated in a thick torus can flow in any direction before it is radiated from the surface. In this disk the flux cannot be neatly separated into radial and vertical components like in the thin α-disk model.

28

3.5 Magnetohydrodynamics (MHD) equation

Many astrophysical phenomena are influenced by the presence of magnetic fields, or even explainable only in terms of magnetohydrodynamic processes. General relativistic MHD is concerned with the dynamics of relativistic, electrically conducting fluids (plasma) in the presence of magnetic fields. Hence the collective interactions between large numbers of plasma particles can isotropize the particle velocity distributions in some local mean reference frame, thereby making it sensible to describe the plasma macroscopically by a mean density, velocity, and pressure. Where this imply that, mean quantities can then be shown to obey the same conservation laws of mass, momentum and energy for fluids. The MHD equations describe conservation of energy, momentum and mass, coupled to the evolution of the magnetic field given by the homogenous Maxwell equation. In four-vector notation this is satisfied by the vanishing four-divergence of the energy-momentum tensor $T^{\mu\nu}$, the mass current density ρu^{μ} and the dual Faraday tensor $F^{*\mu\nu}$ leading to the fundamental relations

$$\nabla_\nu(\rho u^\nu) = 0 \tag{3.5.1}$$

$$\nabla_\nu T^{\mu\nu} = 0 \tag{3.5.2}$$

$$\partial_\mu F_{\nu\lambda} + \partial_\nu F_{\mu\lambda} + \partial_\lambda F_{\mu\nu} = 0 \tag{3.5.3}$$

$$\nabla_\nu F^{\mu\nu} = J^\mu \tag{3.5.4}$$

where $\rho, J^\mu, T^{\mu\nu}$ are mass density, current density and energy momentum tensor respectively. The above equations are conservation law of particle-number, conservation law of energy-momentum and Maxwell equations respectively.

The accreting plasma fluid around kerr black hole induces electromagnetic fields. This electromagnetic field has an effect to perturb the dynamics of the plasma fluid. The flow of a magnetized plasma is most generally described by kinetic theory, general relativity, and Maxwell's equations for the in electromagnetic field. However, many of its features are captured by making two simplifying

assumptions: The plasma particles act like a fluid and the conductivity is so high in the plasma that electric fields generated by free charges are shorted out. Both of these assumptions (which describe the astrophysical plasmas of interest) give rise to the field of study of ideal magnetohydrodynamics.

It is clear that GRMHD comes into play in the innermost region of an AGN. The accretion flow is strongly influenced by the curved rotating space-time. In a first approximation cooling and heating by radiation is neglected. This may be motivated by the fact that the accretion flow moves with relativistic speeds so that radiation cannot significantly influence the flow before it is lost beyond the horizon. Here, we concentrate on purely ideal GRMHD, neglecting the presence of viscosity and heat conduction in the limit of infinite conductivity, i.e., the fluid is assumed to be a perfect conductor. The electromagnetic field in curved space-time is describe by the tensor $F_{\mu\nu}$ as usual.

Since the electromagnetic field (EMF) may or may not conform to the same symmetries as the gravitational field naturally, the problem is greatly simplified by assuming axial symmetry and stationarity for both fields. In the fluid rest frame, the electric field is assumed to vanish completely:

$$F_{\mu\nu}u^\nu = 0$$

By recalling the relation

$$F_{\mu\nu} = \partial\nu A_\mu - \partial\mu A_\nu$$

The relation gives us

$$\frac{A_t,\theta}{A_\phi,\theta} = \frac{A_t,r}{A_\phi,r} = -\omega(r,\theta)$$

where $\omega(r,\theta)$ interpreted as the rotation frequency of electromagnetic field which is vary from flow-line to flow line. This relation imply that,

$$\frac{\omega_{,r}}{\omega_{,\theta}} = \frac{A_{\phi,r}}{A_{\phi,\theta}}$$

. The flow stream-lines and the magnetic field-lines lie in the level surfaces A_ϕ i.e $\vec{a}$ where $B = (^*F).\vec{u}$ and the arrow denotes two-component space-like vectors defined in the (r,θ)-plane. to find

the possible geometry of flow lines, one can introduce the stream function $k(r, \theta)$ satisfying;

$$\frac{u^r}{A_{\phi}, \theta} = -\frac{u^\theta}{A_{\phi}, r} \equiv \frac{k(r\theta)}{4\pi\sqrt{-g}\rho} \tag{3.5.5}$$

apparently, the functional dependence is constrained to $k(r, \theta) \equiv k(A_\phi)$. Therefore magnetic field component are given as;

$$F_{r\phi} = k\sqrt{-g}\rho_o u^\theta \tag{3.5.6}$$

$$F_{\phi\theta} = k\sqrt{-g}\rho_o u^r \tag{3.5.7}$$

$$F_{r\theta} = k\sqrt{-g}\rho_o(\omega u^t - u^\phi) \tag{3.5.8}$$

3.6 Perfect fluid approximation

$$T_{\mu\nu} = \rho h u_\mu u_\nu + p g_{\mu\nu} \tag{3.6.1}$$

$$h \equiv 1 + \epsilon + \frac{p}{\rho} \tag{3.6.2}$$

where ϵ is the specific internal energy density and $T_{\mu\nu}$ boosted from the fluid frame to the eutherian frame (observer). For thermal equilibrium

$$P = p(\rho, \epsilon) \tag{3.6.3}$$

For magnetized fluid

$$F^{\mu\nu} = n^\mu E^\nu - E^\nu n^\mu + n^\mu \epsilon^{\lambda\mu\sigma} B_\sigma \tag{3.6.4}$$

$n \equiv$ observer velocity (Eulerian)

$$E^\mu n_\mu = B^\mu n_\mu = 0 \tag{3.6.5}$$

Assuming the ideal

$$T_{EM}^{\mu\nu} = F^{\mu\lambda}\Gamma_\lambda^\mu - \frac{1}{4}g^{\mu\nu}F_{\alpha\beta}F^{\alpha\beta} \tag{3.6.6}$$

$$b^2 u^\mu u^\nu + \frac{b^2}{2} g^{\mu\nu} - b^\mu b^\nu \quad = \quad T^{\mu\nu}_{EM} \tag{3.6.7}$$

where $b^2 = B^\mu B_\mu$

Conservation equation

$$(\rho u^\mu); \mu \quad = \frac{1}{\sqrt{g}} \frac{\partial}{\partial x^\mu} (\sqrt{g} \rho u^\mu) = \quad 0 \tag{3.6.8}$$

$$T^{\mu\nu}; \nu \quad = \frac{1}{\sqrt{g}} \frac{\partial}{\partial x^\mu} (\sqrt{g} T^{\mu\nu}) = \quad 0 \tag{3.6.9}$$

$$T^{\mu\nu} \quad = \quad (\rho h + b^2) u^\mu u^\nu + (p + \frac{b}{2}) g^{\mu\nu} - B^\mu B^\nu \tag{3.6.10}$$

Chapter 4

Active galactic nuclei interaction on its environment and the resulting dynamics

4.1 Relativistic jets

Astrophysical jets are highly collimated streams of magnetized plasma produced by compact accreting objects. It can be observed in a variety of astronomical sources; among them young stellar objects(YSO), micro-quasars, or active galactic nuclei (AGN). However we focused relativistic jets in AGN. In AGN, relativistic plasma jets are thought to be formed as the result of accretion onto super-massive black-holes (SMBH) in the presence of rotating accretion disks and co-rotating magnetic fields. Relativistic jets transport tremendous amounts of power away from the central region, necessitating them to be coupled with processes involving a SMBH. Therefore potential energy and rotation of the central SMBH are the main power sources for these jets.

Curtis (1918) observe an elliptical galaxy M87 having an odd feature that drawn-out some outflow apparently connected with the nucleus. This outflow was named "jets" by Minkowski and Baade. The commonly accepted model of jets consists of two oppositely directed jets, although in many cases only one side is easily detected. Radio depolarisation measurements are used to determine which jet is pointing towards Earth, with the side with the stronger jet closer to Earth showing less depolarisation since it is viewed through a smaller amount of material along the line-of-sight. AGN in spiral galaxies are unknown as weak radio sources, so it may lead to uncollimated core

Figure 4.1: Relativistic jets in AGN (Credit: Painting by Adolf Schaller for NASA/Goddard Space Flight Center)

sources. Only about 10 percent of radio galaxies (about 0.1 percent of all AGN) are able to launch relativistic jets Begelman and Rees (1984). These jets exhibit structural dimensions far greater than their host galaxies. Jets can be divided in two classes depending on the size of the system: micro jets form in stellar systems whereas macro jets are generated in galactic cores.

The relativistic nature of the most powerful astrophysical objects discovered in active galactic nuclei (relativistic jet) causes them to emit abundant and extremely time variable radiation in all spectral ranges from radio wavelengths to gamma-rays, whereas bulk relativistic motion leads to strong Doppler boosting effects, making them detectable at extreme cosmological distances.

The jet, which originates near an accretion disk that surrounds an AGN, can propagate over a long distance up to a few Mpc while remaining well collimated. There are two shocks at the end of the jet. One is a bow shock (or a forward shock) which accelerates the ambient gas. The other is a terminal Mach shock (or a reverse shock) at which the beam ends. At the terminal Mach shock,

non-thermal particles are accelerated and emit photons due to synchrotron radiation and inverse Compton scattering. The gas which crosses the terminal Mach shock into a hot spot is hottest and pressurized and then expands laterally and envelops the beam with the shocked ambient gas, creating a so-called cocoon structure. At the contact discontinuity between the ambient gas and the jet in the cocoon Kelvin-Helmholtz instabilities develop.

Knots and secondary hot spots are also other active regions in jets. Knots those with nonthermal emission can be seen sporadically along the straight beam flow. The emissivity between the knots varies even if they belong to the same jet. Recent high resolution observations of AGN jets show fine structure of knots in the beam flow for up to several tens of kilo parsecs in M87, 3C273, the jet in Centaurus A and others occurs. Knots on kiloparsec is still not well understood but at parsec or subparsec thought as due to intermittent flows from the central source and in 'blazars' are due to exceptionally strong shocks which are caused by the collisions of internal shocks. The high energy particles that are accelerated on parsec scales may retain their energy for a long time. In some jets, one observes secondary hot spots adjacent to the primary hot spot at the head of jets. The emissivity of secondary hot spot can be as high as that of primary hot spot. It is thought that the gas in the secondary hot spot is separating from the primary hot spot. For example, at both eastern and western side of Cygnus A jet, a bright secondary hot spot is observed. The reason for these multiple hot spots is not well understood.

To comprehend the morphology and the dynamics of the jet,different analytical studies and numerical simulations have been implemented. Most of these relativistic jets (outflows) are morphologically very similar suggesting common physical origin. Their common physical origin are; they differ in size, velocity and amount of energy transport. For instance, in one extreme, AGN jets have typical size greater than $10^6 Pc$, nuclear velocity of the order of light velocity and parent sources (which are massive black holes)with mass $10^{6-9} M_\odot$ and luminosity of about $10^{43-48} erg s^{-1}$ while in other extreme , in young stellar objects, jets have typical size less than $1 pc$, nuclear velocity less 10^3c, and emerge from low mass proto-stars with mass 1MJ and luminosity, $(0.1 - 2 10^4) L_{sun}$.

All jets shared the such common properties, they are:

- Usually collimated to small opening angle and in most cases two-sided

- Originated from the vicinity of compact objects.

- Often terminate in emission lobes (with line emission in the case of young stellar)

- Associated with magnetic fields (the currently most accepted mechanism for jet production).

- Showing evidence of accretion matter onto the central source via an accretion disk.

4.1.1 Relativistic jets formation, acceleration and collimation

The processes by which the jets are accelerated and collimated are still not clearly understood, but it is believed that several of the concepts proposed for extragalactic. However the jet is probably launched by the combined effect of thermal pressure, centrifugal forces, and the Blandford-Znajek process. The major process observed at the center of an AGN is the accretion of disk matter onto the BH. The disk matter is heated and the excessive radiation energy is emitted, due to the viscosity of the accretion disk. Close to the BH, the accretion disk can convert the rest mass-energy of the in-falling matter onto the BH into output energy of either radiation or jets. As a general consensus AGN jets are powered by the accretion disk, the BH rotation, or both of them.

Magnetic fields are a promising agent for jet production because they are abundant in astrophysical plasmas and because the properties of magnetically-powered jets scale trivially with BH mass. However; the generation of this magnetic field around the central black hole by itself is a current strong area of debate by the related field researchers. The mostly consensus is the motion of plasma which rotates onto central compact object. The in-falling plasma fluid has only two velocity components which is used to produce different magnetic field components. These velocity components are radial and azimuthal. The radial motion of charged particles generate toroidal component of the magnetic field while the azimuthal motion generates the poloidal components of the magnetic field. However; as approach to the rotating central black hole, the plasma fluid dominantly acquires the

poloidal magnetic field components due to centrifugal force. The launching mechanism of this relativistic jet is by the collaboration of different ingredients such as; central compact object, accretion disk and magnetic field. The twisted magnetic field lines (due to frame dragging effect of rotating black hole), radiation pressure released by the accreting plasma fluid and the centrifugal force on the accreting plasma fluid are the corner stones of our mechanisms of relativistic jets generation and collimation.

According to the Blandford and Payne (1982) process the angular momentum of a magnetized accretion disk around the collapsed object is the responsible for the acceleration of the plasma. As the poloidal magnetic field is dominant up to the Alfven radius, the field is taken to be frozen into the disk and it enforces an approximate plasma co-rotation similarly to a 'bead on a rotating wire. If the field line forms an angle with the plane of the disk smaller than 60°, the displacements of the plasma from its equilibrium position become unstable. This happens because along these field lines the component of the centrifugal force will be larger than the component of the gravitational force and the plasma will be accelerated outwards. The centrifugal force does not alone accelerate the flow but the opposite and it is its combination with a strong poloidal **B** field that allows for the acceleration. Eventually the acceleration comes from the conversion of Poynting energy flux to kinetic energy flux. The gain in kinetic energy is proportional to the energy that brings the magnetic field lines into rotation. Such a magnetocentrifugal driving mechanism seems to be efficient in disk winds wherein a hot corona is not an absolute requirement. Then, in its origin, the outflow motion has an important equatorial component, while on larger scales the jets are observed to have a motion that is dominantly poloidal.

Penrose process is a principle energy can be extraction from infalling matter of a kerr black hole. Within the ergo-region of a rotating black hole there is negative (redshifted) energy orbits and positive energy, if a particle enters (or exits) the ergosphere. Particles with negative energy orbits must have interacted with other particles prior to this state. When two particles of positive energy interact within the ergo-region, one is propelled into a negative energy orbit, and the other

into a positive energy orbit (through conservation of energy-momentum). If the succeeding positive energy particle exits the ergo-region and escapes the black hole itself, it has extracted energy from the black hole.

The other is BZ mechanism Blandford and Znajek (1999) put forward the possibility of extracting energy and angular momentum from a rotating black hole, to produce electric and magnetic fields and possibly fast outflowing jets. The magnetic field essentially extracts angular momentum from the black hole, reducing its spin. It is plausible that the launching site of jets is in this magnetospheric region around the black hole, powered by the BZ mechanism. First, the rotational energy of the accreting black hole is extracted by a large scale magnetic field accreted onto the black hole, then converted to Poynting flux and finally to relativistic electron/ positron pairs. The main dispute is that the extraction of energy from the black hole through this process is at most as efficient as the extraction of energy from the disk. This only means that the two mechanisms are likely to operate simultaneously. Again this could very well be in favour of a leptonic jet or beam extracted from the back hole embedded in a hadronic heavy wind/jet coming from the disk. Moreover this does not apply necessarily to the gamma ray emission which may still get its energy from the black hole.

The other mechanism of relativistic jet production is which has been applied model to kerr black hole (BZ-mechanism) and to magnetized accretion disk (BP process). This mechanism is known as magnetohydrodynamic (MHD). This mechanism has now been simulated Gammie et al. (2003), ? and is sometimes called the "sweeping pinch" mechanism. The most important ingredient in the MHD mechanism is a magnetic field that is anchored in a rotating object and extends to large distances where the rotational speed of the field is considerably slower. Plasma confined in the magnetic field lines is subject to the Lorentz force, which, under conditions of high conductivity, splits into two vector components: a magnetic pressure gradient and a magnetic tension. Differential rotation between the inner and outer regions winds up the field, creating a strong toroidal component (B_ϕ in cylindrical $[R, Z, \phi]$ coordinates). The magnetic pressure gradient up the rotation axis
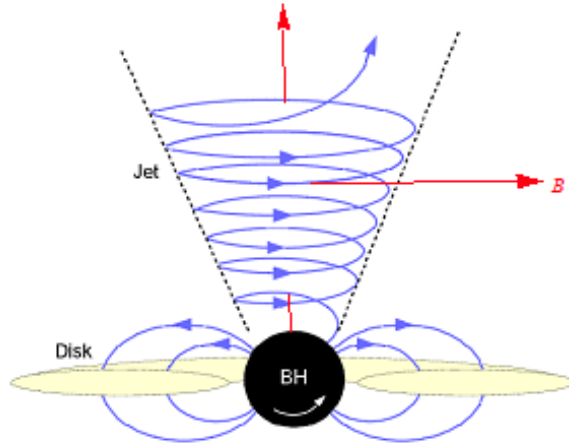
Figure 4.2: Blandford-znajek process

accelerates plasma up and out of the system while the magnetic tension or "hoop" stress $(B_{2\phi}/R)$ pinches and collimates the outflow into a jet along the rotation axis.

Plasma can be extracted from the disk and transported away along the field lines. Then, the outflow originates directly from the accretion flow and is purely centrifugally driven. The outflow speed is comparable to the rotation velocity. Hence, the relativistic outflows can only originate from the innermost part of the accretion disk. The model for the production of jets from accretion disks is relatively well established. It was demonstrated that these are open lines of a poloidal magnetic field, which extend to large distances above the disk surface into the low-density but highly magnetized disk coronae, that can extract the energy and angular momentum of the accreting matter in a form of jets. Such open lines of the magnetic field supported by the infalling gas are anchored within the relatively heavy disk, and so are co-rotating with the accreting matter. A plasma outflow can thus be centrifugally driven from the disk surface into the disk magnetosphere, along the rotating magnetic field lines, with fluid elements moving along the lines like beads on a rotating wire. At some point, the inertia of the outflowing matter starts to play a role, winding up the magnetic field

lines and forming in this way a spiral magnetic structure. The tension and pressure gradient of thus modified magnetic field assures a gradual collimation and bulk acceleration of the fluid elements in the direction perpendicular to the disk surface. As a result, a pair of bipolar jets flowing in opposite directions along the disk normal is formed, converting slowly the initially dominant magnetic flux to the bulk kinetic flux of the carried particles.

Due to frame dragging effect of this rotating black hole twists the poloidal field lines and align them along the azimuthal component. Near by the central gravitating Kerr black hole, plasma fluid keeps on following circular orbit. The twisted poloidal components frozen into this plasma fluid and then in the vicinity of Kerr black hole, the azimuthal (toroidal) magnetic field component is enhanced. This toroidal magnetic field component significantly perturb the dynamics of the plasma fluid.

Once the outflows are accelerated, they will propagate in the form of either collimated beams or uncollimated winds. However, apart for the case of the solar wind, uncollimated flows are hardly observable, while jets are observed in several astrophysical environments, from star formation regions to distant AGN. This is mainly due to the much higher density inside jets as opposed to that in loosely collimated winds. Furthermore, in radio-loud AGN where beams move at relativistic speeds, the emission may be largely amplified by Doppler boosting if the jet is pointed towards the observer, which is probably not the case is radio-quiet sources. Again the two basic mechanisms responsible for collimation may be of thermal or magnetic origin.

If the surrounding medium has a higher pressure than the flow, then an outflow is thermally confined. This implies that there is a pressure gradient forcing the outflow to collimate along its ejection axis. Implication of the above sentences is in general only outflows under-pressured with respect to their surrounding environment may be thermally confined. In fact, such a situation seems to occur in many extragalactic jets, as deduced from X-ray data implying a hot plasma surrounding early-type galaxies and clusters of galaxies.

In general if gravitational field is relatively weak to bound the charges that drifted off from

equatorial plane, the centrifugal force dominates. Therefore the drifted charges excite by the disk surface due to differential rotation, centrifugal force, magnetic hoop stress and radiation force from the accretion disk.

The role of differential rotation is to transport energy and momentum from region of fast rotation to region of slow rotation. Infact accretion disk creates radial and vertical differential rotation. In the case of horizontal differential rotation, the energy and angular momentum transfer outward along the equatorial plane. This arises a sort of radially outward force on the exterior accreting matters. However; the gravitational collapse can balance this effect so that matters keep on accreting. In the case of vertical differential rotation, energy and angular momentum are transported vertical upward above the upper surface of the accretion disk and downward below the lower surface of the accretion disk. Close to Kerr black hole, the effect of differential rotation is pronounced (specially just out side of the ergo-surface). The supply of energy and angular momentum from the plasma fluids in ergosphere is via the outer boundary of the ergosurface. This kicks the particles or the equatorial plane. Supply of energy and angular momentum is sustainable as long as the particles are drifted vertically. The centrifugal force pushes the particles radially out and the magnetic hoop stress does the opposite. Meanwhile, radiation pressure forces the particles along the rotation axis.

4.1.2 Relativistic jet's interaction with the environment

The interest in AGN jet is also relevant due to their role in shaping their host galaxy. During a compact source injects collimated relativistic jets into its cold environment, it is expected that some fraction of the injected power will be dissipated by shocks in the circumstellar gas and dust. AGN jets heat their galactic surroundings, efficiently in the case of FR-I sources and rather inefficiently in the case of the more powerful FR-II sources, which, instead, produce hot cocoons that help protect jets from destructive instabilityFab. After the jet switches off or declines in power, these cocoons may separate to form giant bubbles that rise buoyantly away from the galaxy. They are ultimately assimilated by the circumgalactic medium, which they heat. This is most important when the host

galaxies reside in a rich galaxy cluster.

The parameter that carried out by jets are angular momentum, matter and kinetic and thermal energy. The energy present in the jet, and the presence of both shocks and magnetic field, make them to be a strong candidate for acceleration of particles to the peta-electronvolt (PeV). This could be the source of the far right part of the cosmic ray power spectrum observed on earth. Jets can have a more immediate effect by stimulating star formation as is sometimes seen in some galaxies and, more impressively, by triggering the formation of new galaxies as the jets can propagate several Mpc away from their hosts. Jets also accelerate high energy cosmic rays and quite plausibly may account for a large fraction of the universal spectrum above the knee in the spectrum. They may also be responsible for most of the intergalactic magnetic field. So, AGN play a major role in the evolution of the universe, arguably comparable to that played by stars, and the jets can mediate this interaction directly. Quantitative measures of this role are still quite uncertain and must be compared with the influence of the radiation and outflowing winds that are associated with the accretion disks. All of this must be considered in the young universe when most nuclear activity occurred and massive black holes grew, and even earlier when the intergalactic medium was reionized and the first stars and galaxies were formed.

The other most dynamic fields of the study on relativistic jets, is their role in cosmological models. Since a long time, there exists a inconsistency between observed temperatures of galaxy clusters and the ones predicted from models. The first are higher than the latter. Cosmology needs to feedback energy accreted in objects like galaxies. It is shown that AGN jets have powerful enough luminosity to reheat the cosmological models to the observed temperaturesSilk and Rees (1998). This feedback is now part of most of cosmological models. However the way relativistic jets share their energy with their surroundings is not yet completely understood. However the consensus of diverse mechanisms are thought to be responsible for the energy transfer between the jet and its surroundings. Direct energy conversion takes place at the end of the jet beam, immediately beyond the Mach disk surface of the jet, where kinetic energy becomes thermal energy through efficient

relativistic shocks. Hydrodynamic instabilities taking place at the interface between the shocked jet and shocked ISM matter mix the two fluids, allowing for energy transfer from the now hot outer part of the beam to the surroundings of the jet. In addition a bow shock forms around the entire jet cocoon, propagating in all directions and transferring energy to further regions of space.

4.2 Particle motion equation and radiative transfer

4.2.1 Particle motion

By using line element

$$ds = \sqrt{-g_{\mu\nu}dx^\mu dx^\nu} \tag{4.2.1}$$

and the variational principle is

$$\delta \int ds = 0 \tag{4.2.2}$$

$$0 = \delta \int \sqrt{-g_{\mu\nu}\frac{dx^\mu}{d\tau}\frac{dx^\nu}{d\tau}}d\tau \tag{4.2.3}$$

$$0 = -\frac{1}{2}\int (-g_{\mu\nu}\frac{dx^\mu}{d\tau}\frac{dx^\nu}{d\tau})^{-1/2}\delta(g_{\mu\nu}\frac{dx^\mu}{d\tau}\frac{dx^\nu}{d\tau})d\tau \tag{4.2.4}$$

$$0 = -\frac{1}{2}\int (-g_{\mu\nu}\frac{dx^\mu}{d\tau}\frac{dx^\nu}{d\tau})^{-1/2}\delta(g_{\mu\nu}\frac{dx^\mu}{d\tau}\frac{dx^\nu}{d\tau})d\tau \tag{4.2.5}$$

Multiplying to the right by the factor $(-g_{\mu\nu}\frac{dx^\mu}{d\tau}\frac{dx^\nu}{d\tau})^{1/2}$

$$0 = -\frac{1}{2}\int ((-g_{\mu\nu}\frac{dx^\mu}{d\tau}\frac{dx^\nu}{d\tau})^{1/2})(-g_{\mu\nu}\frac{dx^\mu}{d\tau}\frac{dx^\nu}{d\tau})^{-1/2}$$
$$\delta(g_{\mu\nu}\frac{dx^\mu}{d\tau}\frac{dx^\nu}{d\tau})d\tau \tag{4.2.6}$$

It gives

$$0 = \frac{1}{2}\int \delta(g_{\mu\nu}\frac{dx^\mu}{d\tau}\frac{dx^\nu}{d\tau})d\tau \tag{4.2.7}$$

43

using least action principle

$$s = \int L(\lambda, x, \dot{x})d\lambda \tag{4.2.8}$$

using (4.2.8)and (**??**)

$$\delta \int L d\tau = \frac{1}{2}\delta \int (g_{\mu\nu}\frac{dx^\mu}{d\tau}\frac{dx^\nu}{d\tau})d\tau \tag{4.2.9}$$

This yields

$$L = \frac{1}{2}(g_{tt}\dot{t}^2 + 2g_{t\phi}\dot{t}\dot{\phi} + g_{rr}\dot{r}^2 + g_{\phi\phi}\dot{\phi}^2) \tag{4.2.10}$$

The implication is just as in classical mechanics, we can alternatively take the Lagrangian approach to the equations of motion.

Using Lagrangian the constant of the motion are

$$L = \frac{1}{2}(g_{\mu\nu}p^\mu p^\nu) \tag{4.2.11}$$

For the static and axisyymetry metric $g_{\mu\nu}$ is indepedent of the t and ϕ coordinate. This implies that

$$\frac{\partial L}{\partial x^\mu} = 0 \tag{4.2.12}$$

for t and ϕ

$$\frac{\partial L}{\partial t} = 0 \tag{4.2.13}$$

and

$$\frac{\partial L}{\partial \phi} = 0 \tag{4.2.14}$$

Then by euler-lagrangian equation

$$\frac{d}{d\lambda}(\frac{\partial L}{\partial \dot{x}^\mu}) - \frac{\partial L}{\partial x^\mu} = 0 \tag{4.2.15}$$

$$\frac{d}{d\lambda}(\frac{\partial L}{\partial \dot{t}}) - \frac{\partial L}{\partial t} = 0 \tag{4.2.16}$$

44

it gives

$$\frac{d}{d\lambda}\left(\frac{\partial L}{\partial \dot{t}}\right) = 0 \qquad (4.2.17)$$

By integrating

$$\int \frac{d}{d\lambda}\left(\frac{\partial L}{\partial \dot{t}}\right)d\lambda = constant \qquad (4.2.18)$$

$$\frac{\partial L}{\partial \dot{t}} = -E \qquad (4.2.19)$$

$$\qquad (4.2.20)$$

Along ϕ

$$\frac{d}{d\lambda}\left(\frac{\partial L}{\partial \dot{\phi}}\right) - \frac{\partial L}{\partial \phi} = 0 \qquad (4.2.21)$$

$$\frac{d}{d\lambda}\left(\frac{\partial L}{\partial \dot{\phi}}\right) = 0 \qquad (4.2.22)$$

Now by integrating

$$\int \frac{d}{d\lambda}\left(\frac{\partial L}{\partial \dot{\phi}}\right)d\lambda = constant \qquad (4.2.23)$$

$$\frac{\partial L}{\partial \dot{\phi}} = J_z \qquad (4.2.24)$$

where E and J_z are the total energy of the particle and the projection of its angular momentum along

the black hole spin axis respectively.

The 4-component energy momentum vector p^μ is

$$P^\mu = (P^t, P^r, P^\theta, P^\phi)$$

$$= -p_t, p_r, p_\theta, p_\phi$$

$$-E, p_r, p_\theta, J_z$$

45

$$p_r = g_{rr}p^r = \frac{\rho^2}{\Delta}\dot{r} \tag{4.2.25}$$

$$p_\theta = g_{\theta\theta}p^\theta = \rho^2\dot{\theta} \tag{4.2.26}$$

Along $\dot{t}$

$$\frac{\partial(g_{tt}\dot{t}^2 + 2g_{t\phi}\dot{t}\dot{\phi} + g_{rr}\dot{r}^2 + g_{\phi\phi}\dot{\phi}^2)}{2\partial\dot{t}} = E \tag{4.2.27}$$

This gives

$$E = g_{tt}\dot{t} + g_{t\phi}\dot{\phi} \tag{4.2.28}$$

Along $\dot{\phi}$

$$\frac{\partial(g_{tt}\dot{t}^2 + 2g_{t\phi}\dot{t}\dot{\phi} + g_{rr}\dot{r}^2 + g_{\phi\phi}\dot{\phi}^2)}{2\partial\dot{\phi}} = J_z \tag{4.2.29}$$

$$J_z = -g_{t\phi}\dot{t} + g_{\phi\phi}\dot{\phi} \tag{4.2.30}$$

Now, multiplying the equation(4.2.28) by $-\frac{1}{g_{t\phi}}$ and the (4.2.30) $\frac{1}{g_{\phi\phi}}$ then, add together.

$$g_{\phi\phi}E - g_{t\phi}J_z = (g_{\phi\phi}g_{tt} + g_{t\phi}^2)\dot{t} \tag{4.2.31}$$

Finally

$$\dot{t} = E + \frac{2Mr}{\rho^2\Delta}[(r_2 + a^2)E - aJ_z] \tag{4.2.32}$$

To determine $\dot{\phi}$

$$\frac{1}{g_{tt}}E = \frac{1}{g_{tt}}(g_{tt}\dot{t} + g_{t\phi}\dot{\phi}) \tag{4.2.33}$$

$$\frac{1}{g_{t\phi}}J_z = \frac{1}{g_{t\phi}}(-g_{t\phi}\dot{t} + g_{\phi\phi}\dot{\phi}) \tag{4.2.34}$$

$$\dot{\phi} = \frac{2MarE(\Sigma - 2Mr)L_z\csc^2\theta}{\Sigma\Delta} \tag{4.2.35}$$

46

Let us now derive the equation for the radial component of the four-velocity.

$$L = \frac{1}{2}\mu \tag{4.2.36}$$

where μ, is the rest mass of the particle (equal to 0 for massless particles and -1 for particles with non-zero mass).

$$\frac{1}{2}\mu = \frac{1}{2}(g_{tt}\dot{t}^2 + g_{t\phi}\dot{t}\dot{\phi} + g_{t\phi}\dot{t}\dot{\phi} + g_{\phi\phi}\dot{\phi}^2 + g_{rr}\dot{r}^2 + g_{\theta\theta}\dot{\theta}^2) \tag{4.2.37}$$

so we can rewrite it as

$$\mu = (g_{tt}\dot{t} + g_{t\phi}\dot{\phi})\dot{t} + (g_{t\phi}\dot{t} + g_{\phi\phi}\dot{\phi})\dot{\phi} + g_{rr}\dot{r}^2 + g_{\theta\theta}\dot{\theta}^2 \tag{4.2.38}$$

$$\mu = (g_{tt}\dot{t} + g_{t\phi}\dot{\phi})\dot{t} + (g_{t\phi}\dot{t} + g_{\phi\phi}\dot{\phi})\dot{\phi} + \frac{\rho^2}{\Delta}\dot{r}^2 + g_{\theta\theta}\dot{\theta}^2 \tag{4.2.39}$$

substituting equation (4.2.28) and(4.2.30) in (4.2.39)

$$\dot{r}^2 = \frac{\Delta}{\rho^2}[\mu + E\dot{t} - J_z\dot{\phi} - \rho^2\dot{\theta}^2] \tag{4.2.40}$$

$$\dot{\theta}^2 = \frac{1}{\rho^4}[Q + (E^2 + \mu)a^2\cos^2\theta - J_z^2\cot^2\theta] \tag{4.2.41}$$

$$\tag{4.2.42}$$

where Q is a fourth constant of motion called the Carter constant. We got $\dot{r}, \dot{\theta}$ in square form, potentially making the determination of the signs of $\dot{r}$,and $\dot{\theta}$ particularly at turning points, numerically challenging. **Particle motion in the presence of external forces**

Emission from the accreting material around a Kerr black hole is concern therefore, particle motion in the accretion flow must be considered. So the the external force applicable to accretion flows around black holes is considered. Let we apply the condition of $\dot{\theta} << \dot{r} << \dot{\phi} < \dot{t}$, thus allowing $\dot{r}$ and $\dot{\theta}$ given their negligibility compared to other quantities, to be neglected as a first approximation. The equation of motion of particles under the influence of an external force is

$$\ddot{x}^\mu + \Gamma^\mu_{\rho\sigma} = a^\mu \tag{4.2.43}$$

47

where a^μ is the 4-acceleration per unit mass due to an external force.

conditions

- In supposing that accretion onto rotating black holes (axisymmetry) $\partial\phi = 0$.

- In stationarity case $a^\phi = 0$ and also a given the 4-velocity is everywhere orthogonal to the 4-acceleration, so $(a^\nu U_\nu = 0)$.

- We have taken $\dot{r}, \dot{\theta} = 0$,i.e. particles remain in circular orbits, then it follows that $a^t = 0$.

- To avoid difficulties let set $a^r = 0$, which pointed toward a rotationally-supported flow. where $u^\mu u_\nu =$-1 a^θ can be determined self-consistently, under the assumption of $\dot{\theta} = 0$. This solution corresponds to a flow rotationally supported in the $\hat{r}$ direction and pressure supported in the $\hat{\theta}$ direction.

By plugging the affine connection coefficients into equation of motion, then the the non-trivial momentum equation in the radial direction:

$$
\begin{aligned}
0 &= -(\frac{\rho^2 - 2r^2}{\rho^4})\dot{t^2} + 2(\frac{\rho^2 - 2r^2}{\rho^4})a\sin^2\theta\dot{t}\dot{\phi} \\
&\quad -[r + a^2\sin^2\theta(\frac{\rho^2 - 2r^2}{\rho^4})]\sin^2\theta\dot{\phi^2}
\end{aligned}
\tag{4.2.44}
$$

$$
0 = A[-\dot{t^2} + 2a\sin^2\theta\dot{t}\dot{\phi} + (rA^{-1}\sin^2\theta + a^2\sin^4\theta)\dot{\phi^2}]
\tag{4.2.45}
$$

where $A = \frac{\rho^2 - 2r^2}{\rho^4}$

Finally it gives us

$$
\dot{t} = a\sin^2\theta + \frac{\sqrt{r}\rho^2\sin\theta}{\sqrt{2r^2 - \rho^2}}
\tag{4.2.46}
$$

48

which is exactly related to prograde rotation. This solution allows the flow to match the rotation of a prograde accretion disk. From the metric

$$
\begin{aligned}
1 \;=\; & -(\frac{\rho^2 - 2r^2}{\rho^4})\dot{t}^2 + 2(\frac{\rho^2 - 2r^2}{\rho^4})a\sin^2\theta\,\dot{t}\dot{\phi} \\
& -[r + a^2\sin^2\theta(\frac{\rho^2 - 2r^2}{\rho^4})]\sin^2\theta\,\dot{\phi}^2
\end{aligned} \tag{4.2.47}
$$

By plugging the value of $\dot{t}$, then

$$
1 \;=\; \rho^2\sin^2\theta(\frac{r(\rho^2 - 2r)}{2r^2 - \rho^2} + \frac{2\sqrt{r}a\sin\theta}{\sqrt{2r^2 - \rho^2}})\dot{\phi}^2 \tag{4.2.48}
$$

Finally after algebraic simplification, the four velocity are;

$$
\dot{t} \;=\; \frac{1}{\zeta}(\rho^2\sqrt{r} + a\sin\theta\sqrt{2r^2 - \rho^2}) \tag{4.2.49}
$$

$$
\dot{r} \;=\; 0 \tag{4.2.50}
$$

$$
\dot{\theta} \;=\; 0 \tag{4.2.51}
$$

$$
\dot{\phi} \;=\; \frac{\sqrt{2M(2r^2 - \rho^2)}}{\zeta\sin\theta} \tag{4.2.52}
$$

where

$$
\zeta = \sqrt{\rho^2(\rho^2(r+1) - 4r^2 + 2a\sin\theta\sqrt{r(2r^2 - \rho^2)})}
$$

Now equating equation (4.2.39) and (4.2.50) to get energy and equation(4.2.35) and (4.2.52) gives z-component of the angular momentum of the particle as

$$
\frac{1}{\zeta}(\rho^2\sqrt{r} + a\sin\theta\sqrt{2r^2 - \rho^2}) \;=\; E + \frac{2Mr}{\rho^2\Delta}[(r_2 + a^2)E - aJ_z] \tag{4.2.53}
$$

$$
\tag{4.2.54}
$$

Then, energy is equal to

$$
E \;=\; \frac{1}{\zeta}[(\rho^2 - 2Mr)\sqrt{r} + a\sin\theta\sqrt{2r^2 - \rho^2}] \tag{4.2.55}
$$

and z-component of the angular momentum of the particle is

$$
J_z \;=\; \frac{\sin\theta}{\zeta}[(r^2 + a^2)\sqrt{2r^2 - \rho^2} - 2aMr^{3/2}\sin\theta] \tag{4.2.56}
$$

49

The marginally stable orbit, or innermost stable circular orbit (ISCO), for material particles is determined by the surface where $\frac{\partial E}{\partial r} = 0$,

$$\frac{\partial E}{\partial r} = 0 = \Delta\rho^4 - 4r(\sqrt{2r^2 - \rho^2} - a\sin\theta\sqrt{r})^2 \qquad (4.2.57)$$

In a case $a = 0$, limited to the inner boundary of an accretion disk (which considered as Schwarzschild black hole).

The velocity component of $\dot{\phi}$ is exist only for regions sufficiently far from the black-hole event horizon. The approximation adopted here breaks down when the square root in the denominator (ζ) approaches zero. This occurs at the light circularisation radius r_{circ}, which is given by $\zeta = 0$, or equivalently

$$\rho^2(r + 1) - 4r^2 + 2a\sin\theta\sqrt{r(2r^2 - \rho^2)}|_{r=r_{circ}} = 0 \qquad (4.2.58)$$

The assumption that $\theta = 0$ is invalid for radii smaller than the radius of the marginally stable orbit, where the flow is neither pressure nor rotationally supported and it follows a geodesic into the event horizon.

4.2.2 Radiative transfer equation

The emission, absorption and transport process in a medium is classically given as

$$\frac{dI_v}{ds} \;=\; -\alpha_\nu I_\nu + j_\nu \tag{4.2.59}$$

where $I_\nu(s)$ is the specific intensity of the ray at a frequency ν as function of geodesic element, α_ν and j_ν are, the absorption and emission coefficients of the plasma at a frequency ν respectively and ds is the differential path length. The optical depth of the medium is

$$\tau_\nu(s) \;=\; \int_{s_o}^{s} ds^{'} \, \alpha_\nu(s') \tag{4.2.60}$$

So by equation (4.2.59) and (4.2.60)

$$\frac{dI_\nu}{d\tau_\nu} \;=\; -I_\nu + s_\nu \tag{4.2.61}$$

where we have defined the source s_v as

$$s_v \;=\; \frac{j_\nu}{\alpha_\nu} \tag{4.2.62}$$

Integrating (4.2.62) we obtain

$$I_\nu \;=\; I_\nu(o)e^{-\tau_\nu} + \int_{0}^{\tau_\nu} d\tau'_\nu S_\nu(\tau'_\nu)e^{-(\tau_\nu - \tau'_\nu)} \tag{4.2.63}$$

where the constant $I_\nu(0)$ is the initial value of the specific intensity. The classical radiative transfer we have developed so far is in general not covariant. The general covariant radiative transfer equation can be derived from the basic principles based on the conservation of particles in phase space. Accordingly, the particle number density in the phase volume element

$$f(x,p) = \frac{dN}{d\mathcal{V}} \tag{4.2.64}$$

is an invariant quantity along the affine parameter λ.

On the other hand, by Liouville's theorem the phase space volume is invariant along λ, so that

$$\frac{d\mathcal{V}}{d\lambda} = 0 \tag{4.2.65}$$

where the six dimensional phase-space volume element $d\mathcal{V}$ is given as

$$d\mathcal{V} = d^3\mathbf{x}d^3\mathbf{p} \tag{4.2.66}$$

Now using equations 4.2.64 & 4.2.66, we obtain

$$f(x,p) = \frac{dN}{p^2 dp d\Omega v dA dt} \tag{4.2.67}$$

Where Ω is the spherical solid angle and v is the velocity of the particle flow. For the relativistic particles, obviously $p = E$, the particle energy and $v = c = 1$. Then, 4.2.66 is recast as

$$f(x,p) = \frac{dN}{E^2 dE d\Omega dA dt} \tag{4.2.68}$$

equation 4.2.68 can be given in terms of the relative radiative transfer with respect to that of photons as

$$f(x,p) = \frac{dN}{p^2 dp d\Omega v dA dt} \tag{4.2.69}$$

4.3   General relativistic radiative transfer

$$f = \frac{dN}{E^2 dE dA dt d\Omega} \tag{4.3.1}$$

$$f = \frac{dN}{P^2 dp d\Omega v dA dt d\Omega} \tag{4.3.2}$$

This equation can be transferred to an invariant quantity I given as

$$I = \frac{f}{I_{\nu photon}} \tag{4.3.3}$$

where $I_{\nu photon} \equiv$ the specific intensity of the photons given by Rybick and Lightman (1979).

$$I_{\nu ph} \quad = \quad \frac{EdN}{dAdtdEd\Omega} \qquad (4.3.4)$$

using equation (4.3.2)-(4.3.4) we obtain

$$I \quad = \frac{I_{\nu ph}}{E^3} = \quad \frac{I_\nu}{\nu^3} \qquad (4.3.5)$$

Equation (4.3.5) is used to develop general radiative transfer. The transformation of the absorption coefficient from steariming particles with $\vec{v}$ frame say k to a stationary source say in frame k' is obtained. From the optical depth in response to specific frequency ν, $\tau_\nu = l\alpha_\nu (\alpha_\nu = \frac{l}{I_\nu})$

$$\begin{aligned} \tau_\nu \quad &= \quad \frac{l}{\nu}\alpha_\nu \nu \\ &= \frac{l}{k_\perp}\alpha_\nu \nu \end{aligned} \qquad (4.3.6)$$

where c=1. The quantities l and $k_\perp$ are invariant in both frames, since they are perpendicular to the streaming

$$\alpha_\nu \nu = \frac{\tau_\nu}{l/k_\perp}$$

is a lorentz invariant absorption coefficient.

$$\chi \quad = \quad \alpha_\nu \nu \qquad (4.3.7)$$

On the other hand from the source by equation $\frac{S_\nu}{\nu^3}$ is a lorentz invariant. so that the emission coefficient is just

$$\eta \quad = \frac{S_\nu}{\nu^3}\nu = \quad \frac{j_\nu}{\nu^3} \qquad (4.3.8)$$

Now the coefficient χ and η both by local rest frame and the frame at far point are invariant and thus

$$\chi = \chi_o \Rightarrow \alpha_\nu \nu = \nu_o \alpha_{o\nu} \qquad (4.3.9)$$

$$\eta = \eta_o \Rightarrow \frac{j_{o\nu}}{\nu_o^3} = \frac{j_\nu}{\nu^3} \qquad (4.3.10)$$

53

$$\alpha_\nu = (\frac{\nu}{\nu})\alpha_{o\nu} \tag{4.3.11}$$

$$j_\nu = (\frac{\nu}{\nu})j_{o\nu} \tag{4.3.12}$$

Then the relative energy shift in a moving medium with respect to an observer at infinity for photons

$$\frac{E_o}{E} = \frac{\nu_o}{\nu} = \frac{k_\alpha u^\alpha \mid_\lambda}{k_\beta u^\beta \mid_\infty} \tag{4.3.13}$$

where u^α is defined as 4-velocity of the photon propagation in the fluid. k_α is the 4-momentum of the photon.

Note: The transverse component is the photon 4-velocity, orthogonal to u^α in the co-moving fluid is obtained by projection tensor.

$$p^{\alpha\beta} = g^{\alpha\beta} + u^\alpha u^\beta \tag{4.3.14}$$

$$u^\alpha = p^{\alpha\beta}k_\beta = k^\alpha + (k_\beta u^\beta)u^\alpha \tag{4.3.15}$$

So that the variational of the trajectory with respect to the affine parameter λ is

$$\frac{dI}{d\lambda} = \parallel u^\alpha \parallel \mid_{\lambda obs}$$
$$= \sqrt{g_{\alpha\beta}u^\alpha u^\beta}\mid_{\lambda obs} \tag{4.3.16}$$

using (4.3.15) and (4.3.16)

$$\frac{dI}{d\lambda} = k_\beta u^\beta \mid_{\lambda obs} \tag{4.3.17}$$

For stationary observer located at infinity

$$k_\alpha u^\alpha = E_{obs} \tag{4.3.18}$$

Therefore by equation(4.3.13), (4.3.17) and(4.3.18) the relative energy shift of the photon between the observers and comoving frame is

$$\frac{\nu_o}{\nu} = \frac{k_\beta u^\beta \mid_\lambda}{E_{obs}} = \frac{k_\beta u^\beta \mid_\lambda}{k_\alpha u^\alpha \mid_{obs}} \tag{4.3.19}$$

54

Now the radiative transfer equation in the comoving frame derived along the world line of the particle. so

$$\begin{aligned} \frac{dI}{d\lambda} &= \frac{\partial I}{\partial x^\alpha}\frac{dx^\alpha}{d\lambda} + \frac{\partial I}{\partial k^\alpha}\frac{dk^\alpha}{d\lambda} \\ &= k^\alpha \frac{\partial I}{\partial x^\alpha} + \frac{\partial I}{\partial k^\alpha}\frac{dk^\alpha}{d\lambda} \end{aligned} \tag{4.3.20}$$

For photon the geodesic equation with respect to the affine parameter λ is

$$\frac{dk^\alpha}{d\lambda} + \Gamma^\alpha_{\sigma\varepsilon}k^\sigma k^\varepsilon = 0 \tag{4.3.21}$$

Then using equation (4.3.20) in (4.3.21) implies

$$\frac{dI}{d\lambda} = k^\alpha \frac{\partial I}{\partial x^\alpha} - \Gamma^\alpha_{\sigma\varepsilon}k^\sigma k^\varepsilon \frac{\partial I}{\partial k^\alpha} \tag{4.3.22}$$

Now using the derived set of equation and noting that

$$\frac{dI}{d\lambda} = \left(\frac{dI}{ds}\right)\left(\frac{ds}{d\lambda}\right) \tag{4.3.23}$$

The radiative transfer along the world-line of the particles i.e in the local rest frame of the fluid is

$$\frac{dI}{d\lambda} = -k_\alpha k^\alpha \mid_\lambda \left(-\alpha_{o\nu}I + \frac{j_{o\nu}}{\nu_o^3}\right) \tag{4.3.24}$$

where both $\alpha_{o\nu}$ and $j_{o\nu}$ defined in the fluid rest frame i,e

$$\alpha_{o\nu} = (x^\beta, \nu)$$

$$j_{o\nu} = (x^\beta, \nu) \tag{4.3.25}$$

Finally,(4.3.24) is used to numerically integrate the relativistic radiative transfer where the optical depth is used along, the geodesy of the particle (for photon rays). In the case of massive particles

$$p_\alpha p^\alpha = -m^2 \tag{4.3.26}$$

So that the geodesic equation timelike, then

$$\frac{ds}{d\lambda} = \sqrt{g_{\alpha\beta}[p^\alpha + (p_\beta u^\beta)u^\alpha][p^\beta + (p_\alpha u\alpha)u\beta]} \tag{4.3.27}$$

55

where $u^\beta = p^{\alpha\beta} u_\alpha$ instead of (4.3.15) equation (4.3.27) is simplified to yield

$$\frac{ds}{d\lambda} = \sqrt{(p_\alpha u^\alpha)^2 - m^2} \mid_{\lambda obs} \tag{4.3.28}$$

In similar approach as that of photon, the final radiative transfer equation of massive particles along the world-line of the particle is

$$\frac{ds}{d\lambda} = \sqrt{1 - (\frac{m}{p_m u^\beta \mid_{\lambda obs}})^2} p_\alpha u^\alpha \mid_\lambda (-\alpha_{o\nu} I + \frac{j_{o\nu}}{\nu^3}) \tag{4.3.29}$$

where the energy observed by an observer at infinity is

$$p_\beta u^\beta = E$$

, So that the radiative transfer in the case of massive particles differ by an abberation factor $\sqrt{1 - (\frac{m}{E})^2}$. Hence the intensity gradient along the geodesy is reduced.

4.3.1 Tori supported accretion disk and radiative transfer

$$M_{acc} = \alpha \frac{dM}{dt} = \alpha \dot{M}_{acc} \tag{4.3.30}$$

The accretion rate $\dot{M}_{acc}$ is controlled by the outward momentum transfer from the radiation to the accretion material through scattering and absorption. The limiting case to stop further accreting is determined by the maximum power available from the accreted mass M.

$$L_{plank} = \frac{E_{max}}{t_{min}} = \frac{Mc^3}{r_g} \tag{4.3.31}$$

$$L_{plank} = \frac{c^5}{G} \approx 10^{59} ergs^{-1} \tag{4.3.32}$$

Then the luminosity limit of the radiative power of an object of mass M at equilibrium between radiation and gravity is

$$L_{Edd} = L_{plank} \frac{\Sigma_{grav}}{\Sigma_{rad}} \tag{4.3.33}$$

56

where Σ_{grav} is the object's total effective gravitational cross-section and Σ_{rad} the total radiative cross-section. For standard Eddington limit the the accreting material is mainly assumed to be fully ionized hydrogen, so that the radiation force is exerted mainly on the free electrons through Thomson scattering cross-section as derived by Eddington 1926 given as

$$\dot{M_{Edd}} = \frac{4\pi GMm_p}{c\eta\sigma_T} \qquad (4.3.34)$$

where m_p is proton mass, η is accretion efficient

$$(\eta = \frac{L_{obs}}{L_{acc}} = \frac{L_{obs}}{\dot{M}_{acc}c^2})$$

and σ_T is the Thomson cross-section ($\sigma_T = 6.7 \times 10^{-29}m$)

$$L_{Edd} = L_{plank}\frac{\Sigma_{grav}}{\Sigma_{rad}} = 1.4 \times 10^{38}(\frac{M}{M_\odot}) \qquad (4.3.35)$$

Beyond the Eddington limit, the radiation pressure becomes so large that the thin disk solution no longer holds and the accretion disk puffs up into a torus.

Chapter 5

Result and Discussion

By now the materials and tools developed earlier are being used to address important issues related to AGN effects on its environment.

5.1 The effect of AGN on geometry and dynamics of surrounding systems

5.1.1 Geometrical effect: Kerr geometry and horizon solutions

Recall that

$$ds^2 = g_{\mu\nu}dx^{\mu}dx^{\nu} \tag{5.1.1}$$

This is the invariant line element where the particles basically follow. This metric provides information on the geometry of spacetime around the AGN where all kinematical and dynamical equations are being derived from.

Boundaries, horizons and singularities

These special boundaries are determined by their peculiar characteristics in the metric where they fall under true singularities or coordinate dependent pseudo singularities (horizons) from the form of the metric.

a) The ring singularity:

$$\rho^2 = 0$$

It is obtained at $(r, \theta) = (0, \frac{\pi}{2})$. Its physical meaning is yet unknown. In the limit $a = 0$ this singularity degenerate to schwarzschild peacetime.

b) Coordinate dependent singularities: Event horizons

$$\Delta(r) = 0 \tag{5.1.2}$$

whose horizon solutions are

$$r_\pm = M \pm \sqrt{M^2 - a^2} \tag{5.1.3}$$

where,

r_+ represents the black hole event horizon, while r_- represents the Cauchy event horizon. when $a = 0$, r_+ readily reduced to the Schwarzschild radius, $r_+ = r_{Sch} = \frac{2Gm}{c^2}$, while the r_- is degenerated to the zero true singularity of Schwarzschild black hole.

Matters or events that happen in the cauchy horizon will not affect physics outside of it, i.e in the rest of the Universe. Since, particles in the region $r < r_-$ may never enter the region $r > r_+$.

c) The static limit of Kerr geometry

Also another important Kerr geometry is the boundary regions where ds^2 changes sign. It is located at $g_{tt} = 0$ whose horizons solutions are given as

$$r_{SL\pm} = M \pm \sqrt{M^2 - a^2 \cos^2 \theta} \tag{5.1.4}$$

The solutions of the Kerr geometry are displayed as in the figures below, where we have displayed with different orientations and cross-section cuts for better views.
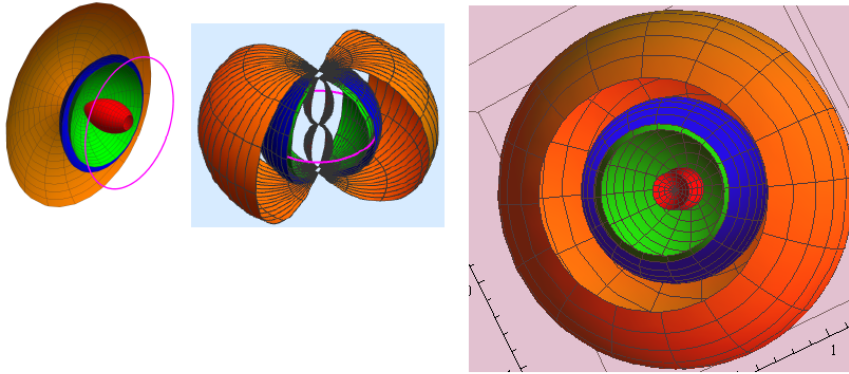
Figure 5.1: The horizon solutions of the Kerr geometry displayed with different orientations and cross-section cuts for better views.

When $\theta = 0$ (at the pole) or $\theta = \pi$, $r_{SL+} = r_+$. In the inner static limit (r_{SL-}) the observer is time like geodesic with $k^\mu = (1, 0, 0, 0)$. The observer must move with the rotation of the Kerr black hole in order to remain timelike in this inner static limit. This region of course defines the inner edge of the ergosphere that lies within the event horizon and is cauchy disconnected from the outside universe.

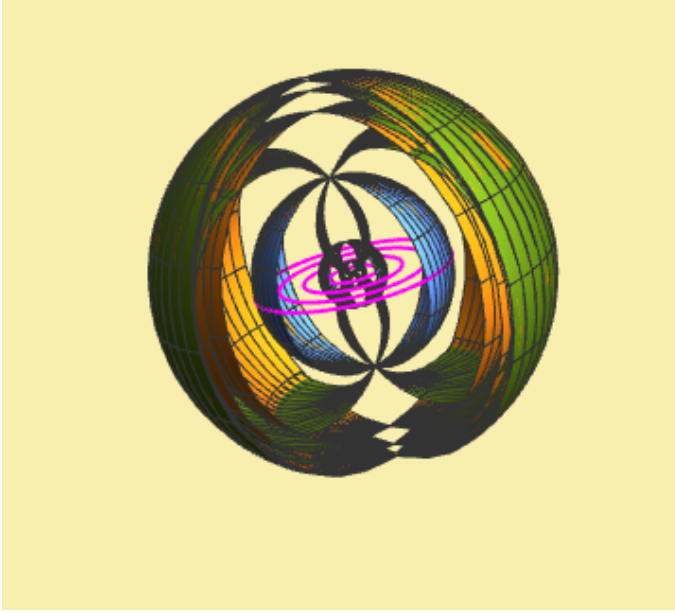For a various values of a the horizons displayed as in the figure

Figure 5.2: Horizon for different value of a

5.2 The effect of kerr geometry on geodesy

From the lagrangian we derived the equations of motion particles, of that free and in presence of external force in the Kerr space-time. Also the constant of motion (i,e energy(E), and angular momentum (J_z)) were derived. All equations derived above are the most important in the observation case. An observer with a fixed spatial coordinate has world line orthogonal to the surface of constant line (the observer zero angular momentum)

$$(u^\mu)_{ZAMO} = (u^t, 0, 0, 0) \tag{5.2.1}$$

in schwarzschild

$$u^\phi = 0$$

in the case of kerr of in BL coordinates for $L_z = u^\phi$

$$
\begin{aligned}
u^\phi &= g^{\phi\alpha}u_\alpha \\
&= g^{\phi t}u_t + g^{\phi\phi}u_\phi
\end{aligned}
\tag{5.2.2}
$$

Then,the geodesy of ZAMO has non zero angular velocity

$$
\begin{aligned}
\Omega \;\; = \frac{d\phi}{dt} = \;\; \frac{d\phi}{d\tau} \Big/ \frac{dt}{d\tau} \\
= \frac{u^\phi}{u^t}
\end{aligned}
\tag{5.2.3}
$$

$$
\Omega \;\; = \;\; \frac{(\frac{g_{t\phi}}{\Delta \sin^2 \theta})u^t}{g^{tt}u_t}
\tag{5.2.4}
$$

where

$$
u^t \;\; = g^{t\alpha}u_\alpha = \;\; g^{tt}u_t + g^{t\phi}u_\phi
\tag{5.2.5}
$$

Therefore

$$
\Omega \;\; = \;\; [\frac{g_{t\phi}}{\Delta \sin^2 \theta}][\frac{\Delta \sin^2 \theta}{g_{\phi\phi}}]
\tag{5.2.6}
$$

$$
\Omega \;\; = -\frac{g_{t\phi}}{g_{\phi\phi}} = \;\; -\frac{\frac{2aMr\sin^2\theta}{\rho^2}}{\frac{\sin^2\theta}{\rho^2}(r^2 + a^2 - \Delta a^2)}
\tag{5.2.7}
$$

$$
\Omega \;\; = \;\; \frac{2Mar}{(r^2 + a^2) - \Delta a^2 \sin^2 \theta}
\tag{5.2.8}
$$

Recall that direction of the rotation of the BH is along J, this implies Ω and J have the same sign. The ZAMo of observer (initial observer) coordinate with the BH. The inertial frame being dragged.

Kerr geometry result in the frame dragging

Then

$$
(u^\mu)_{ZAMO} = (u^t, 0, 0, u^\phi)
$$

$$
u_t \;\; = g_{t\alpha}u_\alpha = \;\; g_{tt}u^t + g_{t\phi}u^\phi
\tag{5.2.9}
$$

using (5.2.7) and(5.2.9)

$$
u_t \;\; = \;\; (g_{tt} - \frac{(g_{t\phi})^2}{g_{tt}})u^t
\tag{5.2.10}
$$

Using normalization condition

$$u^\alpha u_\alpha \;\; = \;\; -1 \tag{5.2.11}$$

$$u^t u_t + u^r u_r + u^\theta u_\theta + u^\phi u_\phi \;\; = \;\; -1 \tag{5.2.12}$$

$$u^t u_t \;\; = -1 = \;\; u^t (g_{tt} - \frac{(g_{t\phi})^2}{g_{tt}}) u^t \tag{5.2.13}$$

$$(u^t)^2 \;\; = \;\; -(g_{tt} - \frac{(g_{t\phi})^2}{g_{tt}}) \tag{5.2.14}$$

$$u^t \;\; = \;\; (-\frac{g_{\phi\phi}}{g_{tt}} - g_{t\phi}^2)^{1/2} \tag{5.2.15}$$

$$u^t \;\; = \;\; \frac{g_{\phi\phi}}{\Delta \sin^2 \theta} \tag{5.2.16}$$

In general

$$(u^\mu)_{ZAMO} \;\; = \;\; \frac{g_{\phi\phi}}{\Delta \sin^2 \theta}(1,0,0,0) \tag{5.2.17}$$

5.3 Correlation between accretion and source of energy release from Astrophysical object

One of the important powerful technique in the observation is the extracting of the data in the form of energy spectra in the form of EM. Thanks to the dedicated scientific communities today also we have possible extraction of gravity energy in the form of Gravitational wave (GW) to mainly the energy released from exotic astrophysical system like accreting compact objects (neutron stars, white dwarf, Black hole) and AGN are in significantly in EM form. The source of energy release

case 1 stellar evolution:Significantly dominated by nuclear reaction

case 2 Exotic objects like Black hole,White dwarf,Neutron star, and AGN - Both nuclear energy and gravitational energy are due to accretion.

i) Contribution from nuclear reaction

If any of these system accretes say dM then, the amount of energy converted to nuclear energy is by mass-energy conversion is given by:

$$dE_n = \alpha dM_{acc} c^2 \tag{5.3.1}$$

where $\alpha \equiv$ conversion factor. In fact the predominant conversion comes from hydrogen. So if we suppose

$$\alpha = \alpha_H + \alpha_{He} + \alpha_c... \tag{5.3.2}$$

$$\alpha \approx \alpha_H \approx 0.007 \tag{5.3.3}$$

Then using equation (5.3.1),(5.3.2) and (5.3.3) we obtain

$$dE_n = 0.007 dM_{acc} c^2 \tag{5.3.4}$$

ii) Contribution from gravity It is in the form gravitational potential energy. So if we assume centering accreting system is mass M, then

$$dE_g = \frac{GM dM_{acc}}{R} \tag{5.3.5}$$

The energy radiated per unit area per unit time is

$$
\begin{aligned}
\frac{dE_{tot}}{A dt} &= \frac{1}{A}\left(\frac{dE_n}{dt} + \frac{dE_g}{dt}\right) \\
&= \frac{1}{A}\left(\frac{GM}{r}\frac{dM}{dt} + 0.007\frac{dM_{acc} c^2}{dt}\right) \\
&= \frac{1}{A}\left(\frac{GM}{R} + 0.007 c^2\right)\dot{M}_{acc} \tag{5.3.6}
\end{aligned}
$$

In general for the gravitating system the source of the energy released from their surface is dominated by gravity due to acceleration and nuclear reaction. For dimensionless parameters let
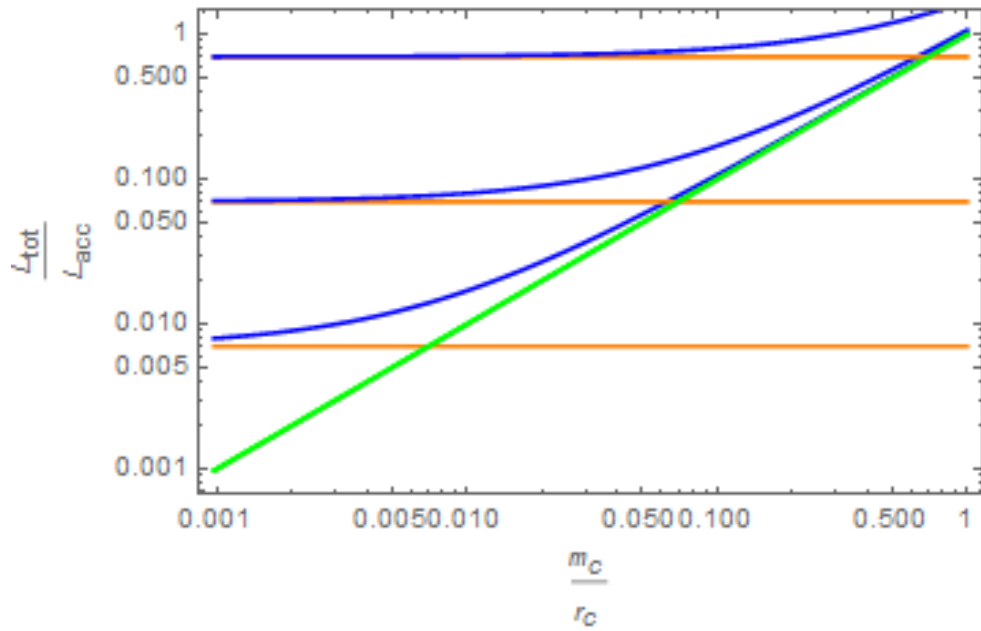
$$m = \frac{M}{M_\odot}$$

Figure 5.3: total luminosity of central gravitating system

the relative mass of the central accreting system to solar

$$r_c = \frac{R}{R_{\odot}}$$

the relative radius of the central accreting system with respect to the solar schwarzschild radius. The figure shown (5.3) the LogLogPlot of the total luminosity released from the central gravitating system relative to the accretion luminosity vs the relative ratio of the central mass system with respect solar mass to its radius with respect solar Schwarzschild radius.

5.4 Radiative transfer in pressure supported torus

In order to calculate accretion from accretion torus the boundary surface and its physical conditions is reasoning. In the case of our system the AGN core are rotating, so that it imposes the condition that a 4-acceleration fluid being support by total ressure is required. However this rotation support model is not sufficient to incorporate the sourrounding atmosphere with optical depth gradient. Thus preferable the pressure supported torus system that includes both the gas pressure and radiation pressure is considered. moreover internal density and temperature effects are considered. Thus the perfect fluid stress-energy-momentum tensor $T^{\alpha\beta}$ of the fluid is

$$T^{\alpha\beta} = (p + \epsilon + \rho)u^{\alpha}u^{\beta} + pg^{\alpha\beta} \tag{5.4.1}$$

where p, ρ, ϵ, are pressure,the fluid internal energy, the density respectively. Applying conservative of $T^{\alpha\beta}$ and then projecting the resulting equation onto the 3-surface orthogonal to the fluid velocity u^{α} with the projection tensor

$$p^{\alpha\beta} = g^{\alpha\beta} + u^{\alpha}u^{\beta}$$

yields the momentum equation

$$(p + \epsilon + \rho)u^{\alpha}_{;\beta}u^{\beta} + p_{;\beta}g^{\alpha\beta} = 0 \tag{5.4.2}$$

Now applying the axisymmetry conditions we have the quantities

$$\Omega = \frac{u^{\phi}}{u^{t}} \tag{5.4.3}$$

$$l = -\frac{u_{\phi}}{u_{t}} \tag{5.4.4}$$

Then the gradient of l is

$$\partial_{\alpha}l = \frac{u_{\phi}}{u_{t}^{2}}\partial_{\alpha}u_{t} - \frac{1}{u_{t}}\partial_{\alpha}u_{\phi} \tag{5.4.5}$$

$$u^{\phi}u_{t} = \Omega(u^{t}u_{t}) = \frac{\Omega}{1 - l\Omega} \tag{5.4.6}$$

Now using equation (5.4.4),(5.4.4),(5.4.5) and (5.4.6) in equation (5.4.1) we obtain the fundamental equation

$$\frac{\partial_\alpha p}{p + \rho + \epsilon} \quad = \quad \partial_\alpha \ln(u_t) - \frac{\Omega \partial_\alpha l}{1 - l\Omega} \tag{5.4.7}$$

which can be numerically integrated based on boundary conditions.

Chapter 6

conclusion

AGNs produce an enormous amount of energy that is injected into their surrounding environment through ionizing radiation and relativistic jets. One of the key roles in the framework of galaxy formation is the AGN activity.

AGN are important astrophysical systems, where their feedbacks in the form of radiative pressure produce self-regulating process which links the energy released from them to the surrounding gaseous medium, impacting on the evolution of the host galaxy. In general the AGNs are amongst the most important astrophysical systems being used in astrophysical studies that require diverse areas of physics.

Successfully developed techniques enables us to understand about effect of AGN on their environment in the framework of General Relativity and General Relativistic Magnetohydrodynamics in a geometry of oblate spheroidal. This takes place in the presence of kerr-metric. These methods are generally incorporate with radiative transfer which is applicable to studies of radiation transport. The equations of motion for particles in the given metric were derived. The flat disk These are used to determine the kinematic properties of the accretion. The derived equations are expected to correlate the process occurred at emission to that of observation point far away from the AGN by the general covariant transformation.

References

Aird, J., Coil, A. L., Moustakas, J., Blanton, M. R., Burles, S. M., Cool, R. J., Eisenstein, D. J., Smith, M. S. M., Wong, K. C., and Zhu, G.: 2012, *The Astrophysical Journal* **746(1)**, 90

Antonucci, R.: 1993, *Annual Review of Astronomy and Astrophysics* 31

Bahcall, J. N. and Spitzer Jr, L.: 1969, *The Astrophysical Journal*

Begelman, M. C., B. R. D. and Rees, M. J.: 1984, *Reviews of Modern Physics* 56(351)

Best, P. N. and Heckman, T. M.: 2012, *MNRAS* **421**, 1569

Blandford, R. and Payne, D.: 1982, *Monthly Notices of the Royal Astronomical Society* **199(4)**, 883

Blandford, R. D. and Znajek, R. L.: 1999, *MNRAS* **(179)**, 433

Blustin, A., Page, M., Fuerst, S., Branduardi-Raymont, G., and Ashton, C.: 2005, *Astronomy & Astrophysics* **431(1)**, 111

Caputi, K. I.: 2014a, *International Journal of Modern Physics D.*

Caputi, K. I.: 2014b, *International Journal of Modern Physics D* **23**, 1430015

Curtis, H. D.: 1918, *Lick Observatory* **13**, 42

Dultzin-Hacyan, D., Krongold, Y., Fuentes-Guridi, I., and Marziani, P.: 1999, *The Astrophysical Journal Letters* 513(2)

Einstein, A.: 1915, *Proceedings of The Prussian Academy of Sciences* **2**, 884

Ellingson, E., Yee, H., and Green, R.: 1991, *The Astrophysical Journal* 371

Fanaroff, B. and Riley, J.: 1974, *Monthly Notices of the Royal Astronomical Society* 167

Fath, E. A.: 1909, *Astronomical Society of the Pacific* **21**, 138

Fisher, K. B., Bahcall, J. N., Kirhakos, S., and Schneider, D. P.: 1996, *arXiv preprint astro-ph/9602078*

Gammie, C. F., McKinney, J. C., and Tóth, G.: 2003, *The Astrophysical Journal* **589(1)**, 444

Gaspari, M.: 2015, *IAU General Assembly* **22**, 2257833

Hickox, R. C., Jones, C., Forman, W. R., Murray, S. S., Kochanek, C. S., Eisenstein, D., Jannuzi, B. T., Dey, A., Brown, M. J., Stern, D., et al.: 2009, *The Astrophysical Journal* **696(1)**, 891

Hill, G. J. and Lilly, S. J.: 1991, *The Astrophysical Journal* **367**, 1

Kharb, P., Lister, M., and Cooper, N.: 2010, *The Astrophysical Journal* **710(1)**, 764

Krolik, J. H.: 1999, *Active galactic nuclei: from the central black hole to the galactic environment*, Princeton University Press

Lanzuisi, G., Ponti, G., Salvato, M., Hasinger, G., Cappelluti, N., Bongiorno, A., Brusa, M., Lusso, E., Nandra, P., Merloni, A., et al.: 2014, *The Astrophysical Journal* **781(2)**, 105

Markarian, B. E.: 1967, *Astrofzika* **3(24)**, 38

Matthews, T. and Sandage, A.: 1963, *Astrophysical Journal* 138

Minkowski, R. and Baade, W.

Mizuta, A., Yamada, S., and Takabe, H.: 2004, *The Astrophysical Journal* **606(2)**, 804

Nixon, C. J., King, A. R., and Price, D. J.: 2012, *MNRAS* **422**, 2547

Schwarzschild, K.: 1916, *Proceedings of The Prussian Academy of Sciences* pp 189–196

Seyfert, C. K.: 1943, *ApJ* **28**, 97

Silk, J. and Rees, M.: 1998, *Astronomy and Astrophysics, 331*

Tewari, B.: 1988, *Astrophysics and space science* **149(2)**, 233

Urry and Padovani: 1995, *Astronomical Society of the Pacific* 107

Weedman, D. W.: 1973, *Astrophysical Journal* 183

Yee, H. and Green, R. F.: 1984, *The Astrophysical Journal* **280**, 79

Zwicky, I. F.: 1967, *Astrofzika* 3

DECLARATION

I hereby declare that this M.Sc thesis is my original work and has not been presented for a degree in any other University and that all source of materials used for the dissertation have been duly acknowledged.

Name: Abdissa Tassama Emana

Signature: _ _ _ _ _ _ _ _ _ _ _ _ _ _ _ _

email:yomiyuglt@gmail.com

This M.Sc dissertation has been submitted for examination with my approval as University advisor.

Name:Dr. Tolu Biressa

Signature: _ _ _ _ _ _ _ _ _ _ _ _ _ _ _ _ _ _

Place and date of submission:

Department of Physics

Jimma University

June, 2019

JIMMA UNIVERSITY
COLLEGE OF NATURAL SCIENCES
PERFORMANCE CERTIFICATE FOR MASTER'S DEGREE

Name of Student: **Abdissa Tassama Emana**   ID No.   **RM1043/10**

Graduate Program: **Regular, M.Sc.**

  1. Course Work Performance

Course Code	Course Title	Cr. hr	Number Grade	Rank **	Remark
Phys691	**M.Sc. Thesis**	**6**			

** Ecellent, Very Good, Good, Satisfactory, Fail.

Thesis Title

Active galactic nuclei activities and flow of relativistic jets

  2. Board of Examiners decision Mark × in one of the boxes. Pass ☐ Failed ☐

If failed, give reasons and indicate plans for re-examination.

_____

_____

  3. Approved by: Name and Signature of members of the examining Board, and Department Head

Committee member	Name	Signature	Date
Chairman	_____	_____	_____
External Examiner	_____	_____	_____
Internal Examiner	_____	_____	_____
Major Advisor	_____	_____	_____

_____   _____   _____
Department head   Signature   Date